Kraftsensorer

- Linear Variable Differential Transformer
- Ofte komplekse sensorer (f.eks. kraft til forskyvning + posisjonssensor)

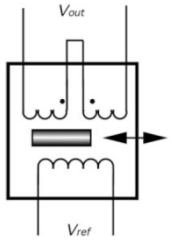

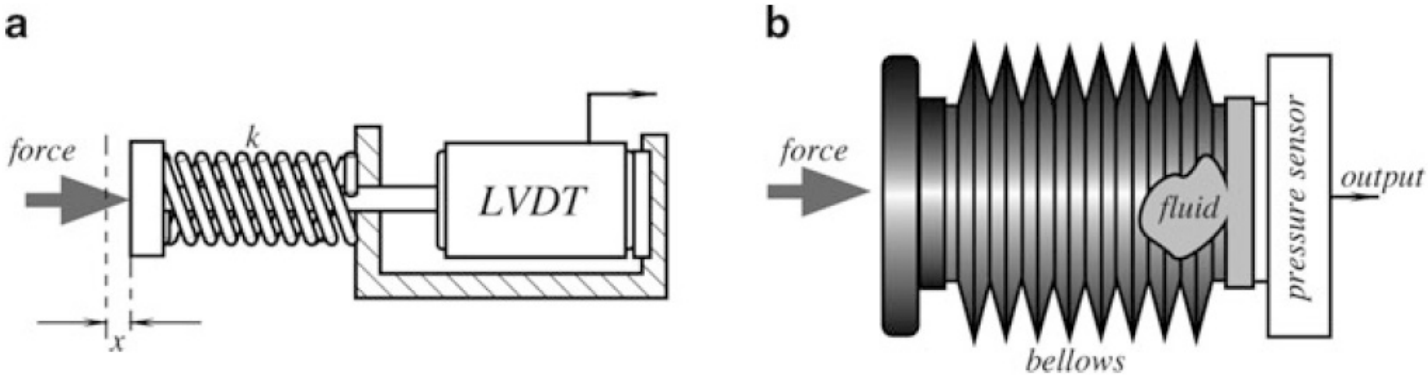

Fig. 9.1 Spring-loaded force sensor with LVDT (**a**). Force sensor incorporating a pressure sensor (**b**)

The various methods of sensing force can be categorized as follows [2]:

1. By balancing the unknown force against the gravitational force of a standard mass
2. By measuring the acceleration of a known mass to which the force is applied
3. By balancing the force against an electromagnetically developed force
4. By converting the force to a fluid pressure and measuring that pressure
5. By measuring the strain produced in an elastic member by the unknown force

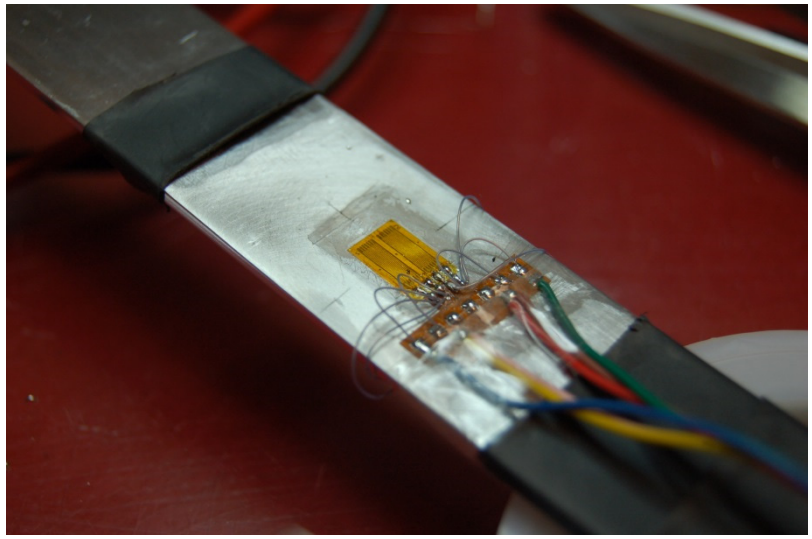

Strekklapp

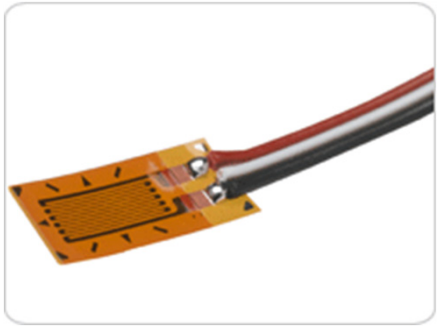

- Piezoresistive materialer
- R øker med strekk og avtar med sammenpressing
- Ofte ganske temperaturfølsomme (noe som må kompenseres for)

Quarter-bridge strain gauge circuit

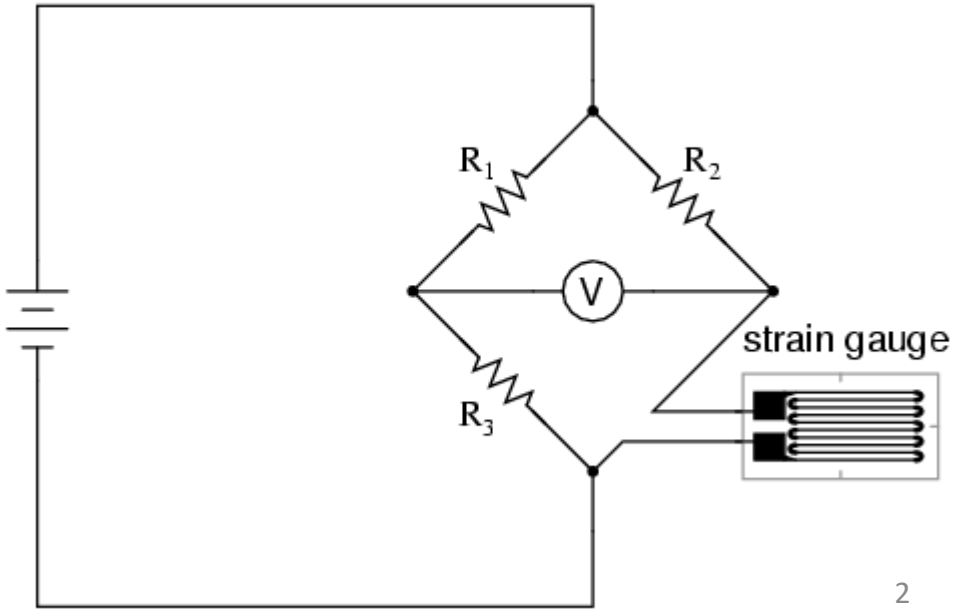

Berøringssensorer

- Tre typer:
  - Touch sensorer (brytere)
  - Spatial sensors (måler fordeling av trykk over en flate)
  - Slip sensors (måler et objekts bevegelse i fht sensoren – at objektet glipper ut av f.eks. et mekanisk grep på en robot)
- Ofte flate paneler

Piezoelektrisk eller piezoresistivt materiale

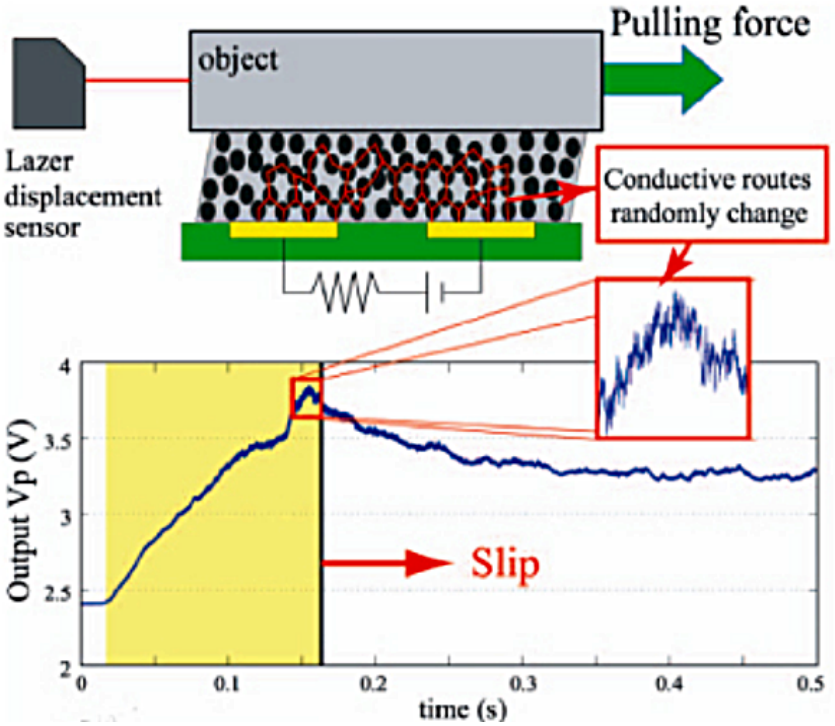

Berøringssensorer

- Touch-type

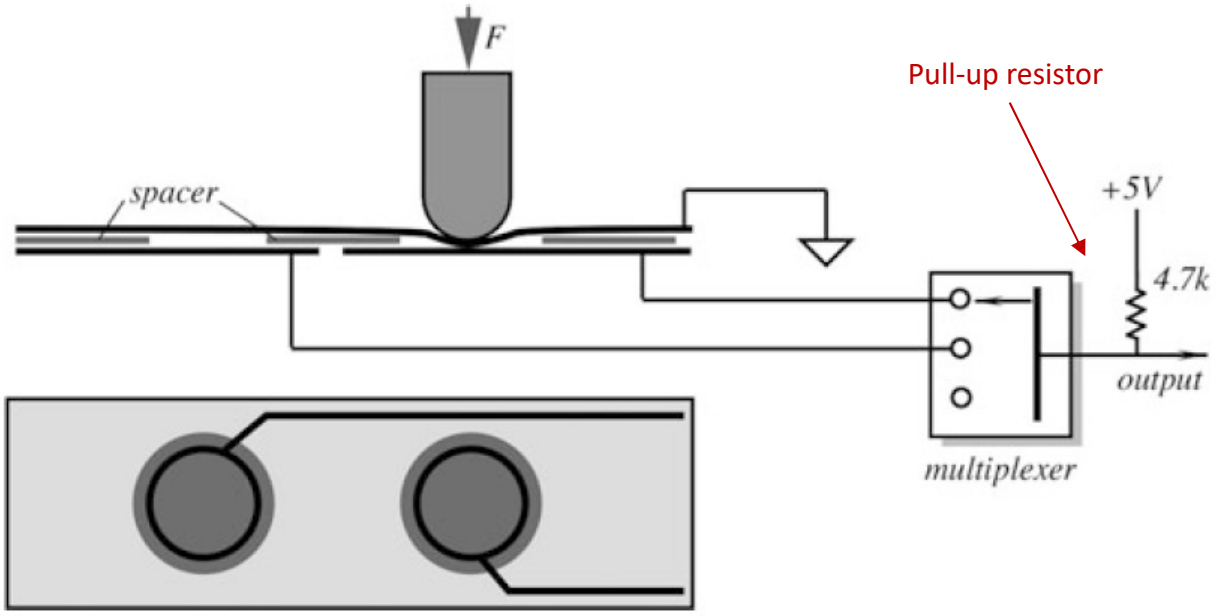

Fig. 9.3 Membrane switch as a tactile sensor

Piezoelektrisk sensor

- Polyvinylidene fluoride (PVDF)
- Nederste film genererer vibrasjoner
- Øverste film genererer spenning
- Når man trykker endres koblingen og dermed signal og fase på utgangen
- Kan lages i celle-mønster for bestemmelse av trykksted (multiplekset utgangssignal)

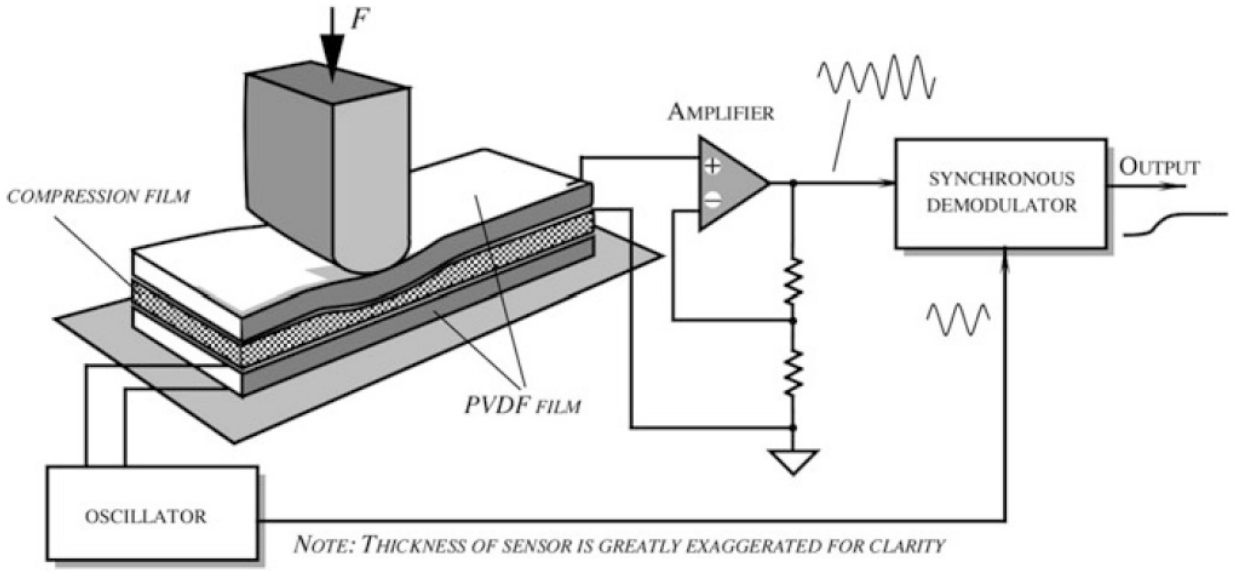

Fig. 9.4 Active piezoelectric tactile sensor

Robotfinger-sensor

- Væskefylt ”underlayer”
- Kan føle ujevnheter ned til 50 µm
- Passiv sensor (ingen eksitasjonsspenning)

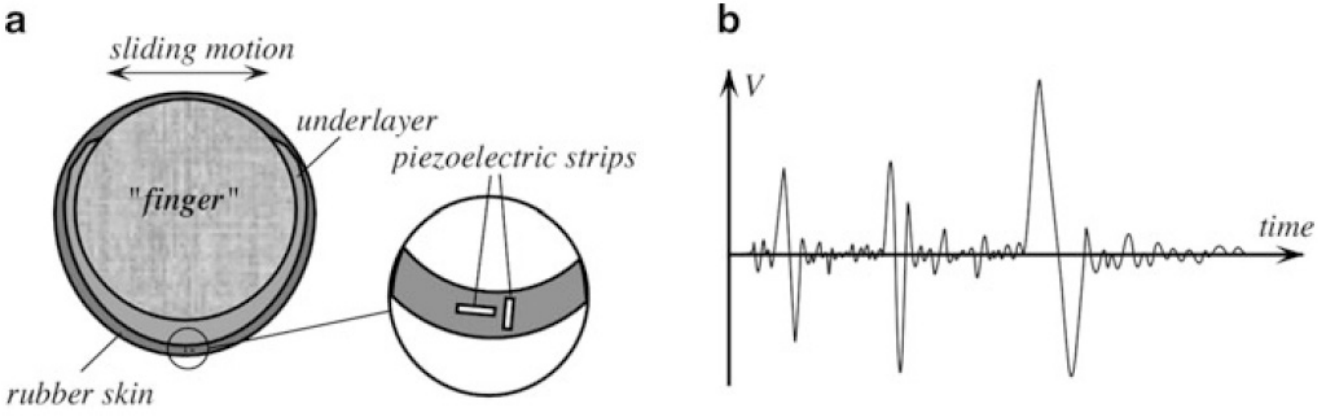

Fig. 9.5 Tactile sensor with a piezoelectric film for detecting sliding forces cross-sectional view (**a**); typical response (**b**) (adapted from [5])

Respirasjons-deteksjon

- Forskyvning av tyngdepunkt

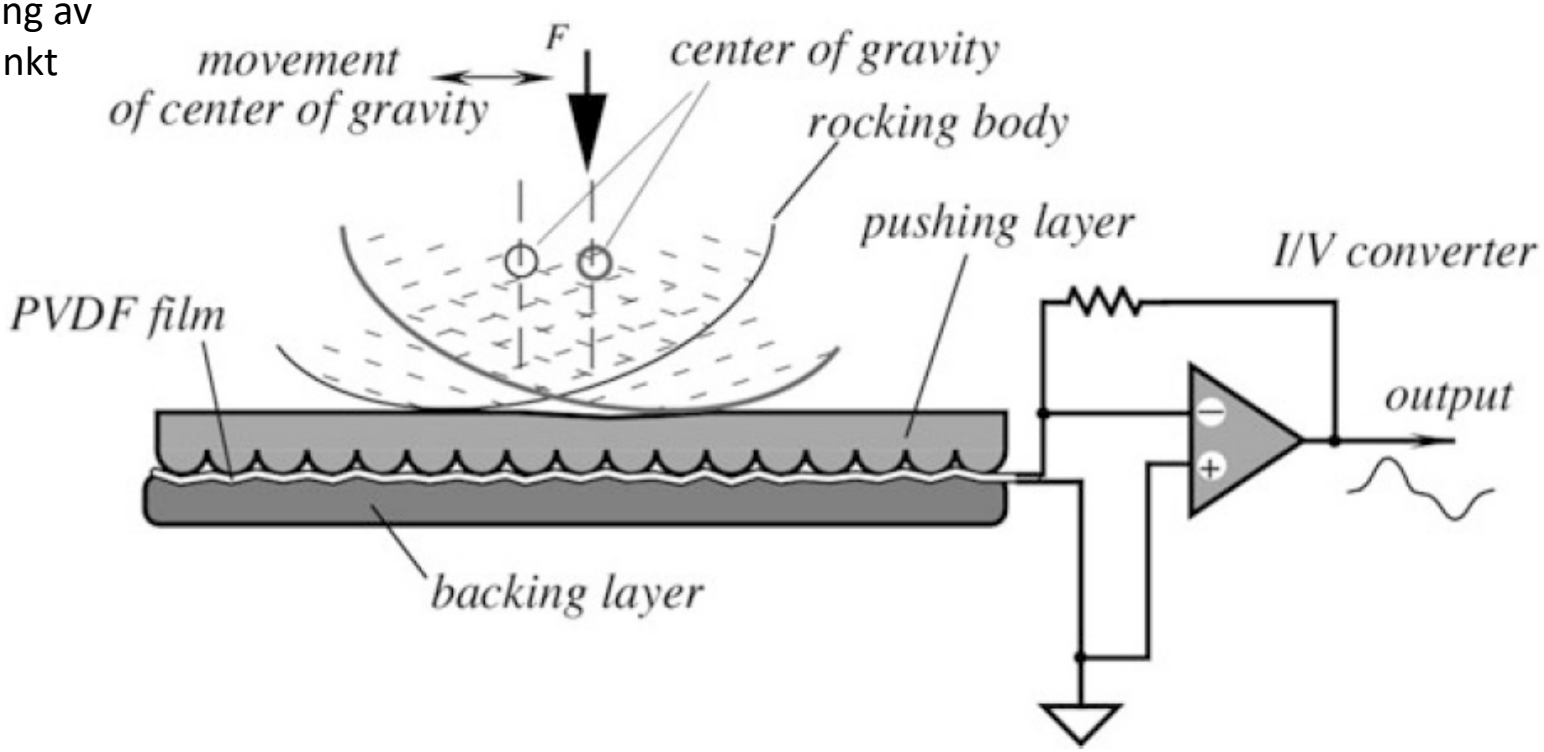

Fig. 9.7 Piezoelectric film respiration sensor

http://video.mit.edu/watch/revealing-invisible-changes-in-the-world-13649/

Trykk-følsom motstand

- Force Sensitive Resistor (FSR)
- Delvis ledende elastomer

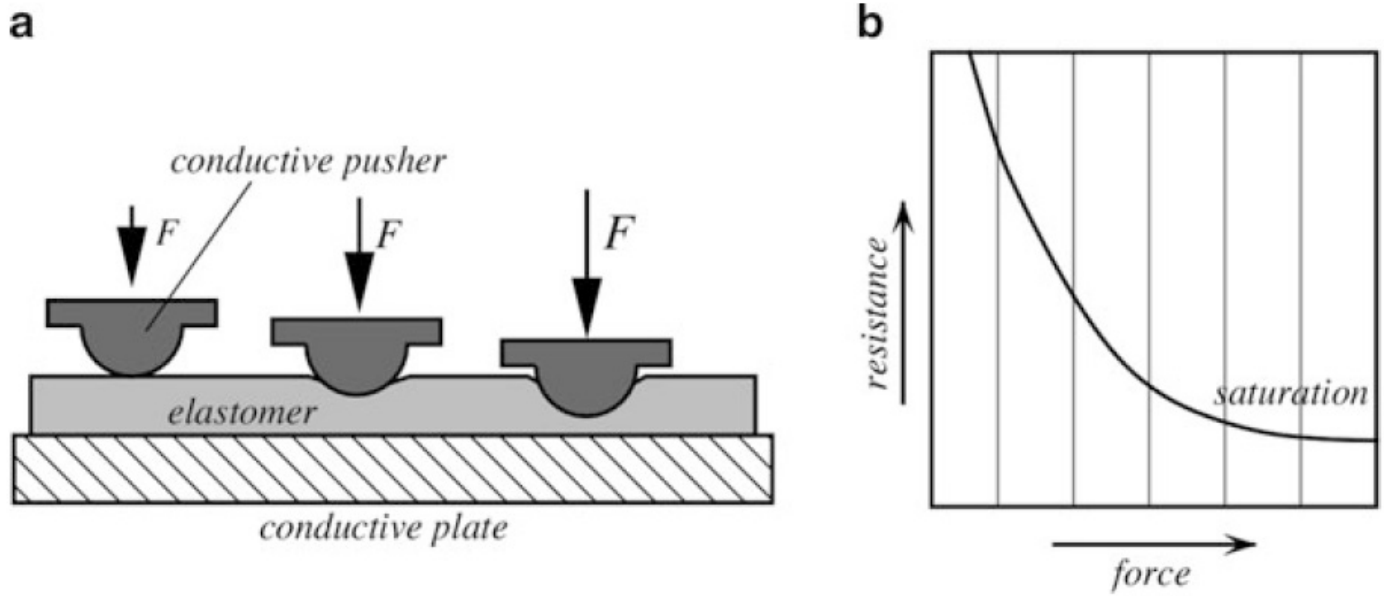

Fig. 9.8 FSR tactile sensor through-thickness application with an elastomer (**a**); transfer function (**b**)

Tynnere FSR

- Tynnere (typ 0,25 mm), større dynamisk måleområde (R varierer over 3 dekader ved 0 – 3 kg), men lavere nøyaktighet (typ ± 10 %), polymer med trykkavhengig resistans

Fig. 9.9 Tactile sensor with a polymer FSR

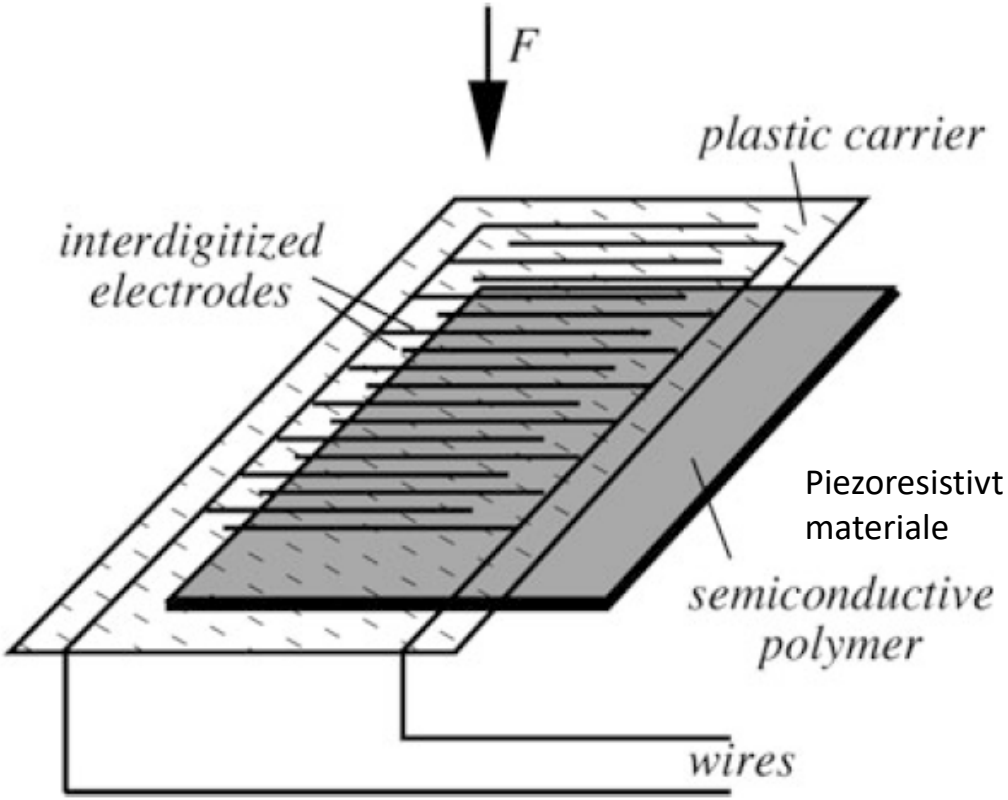

Kapasitive sensorer

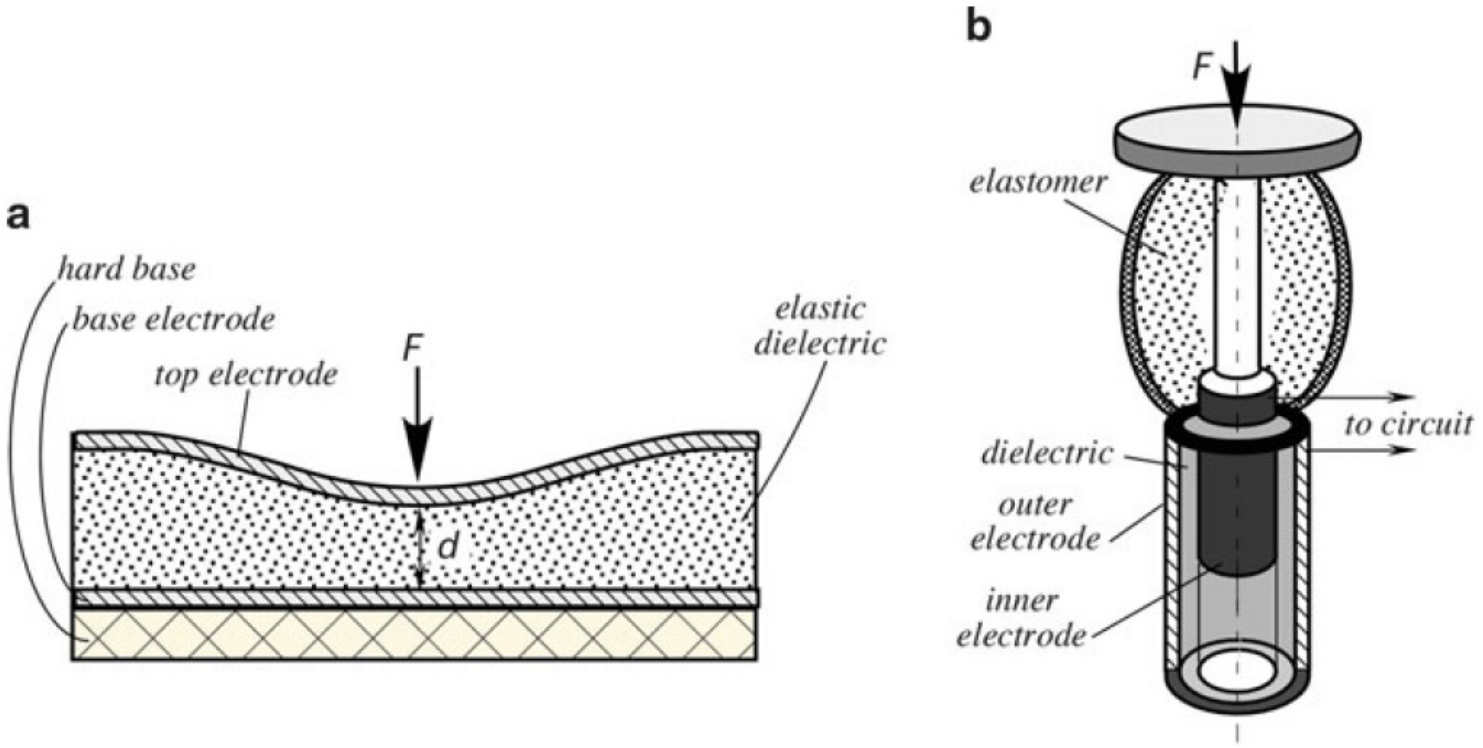

Fig. 9.12 Capacitive tactile sensors. Parallel-plate sensor (**a**) and coaxial sensor (**b**)

Fig. 9.13 Interdigitized and single electrodes for a touch screen

(neste slide …)

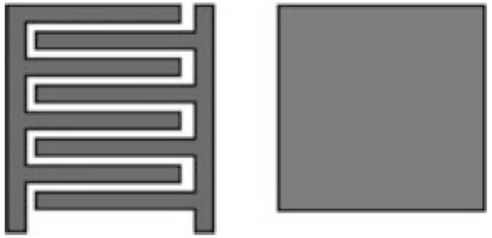

Kapasitiv berøringsfølsom skjerm

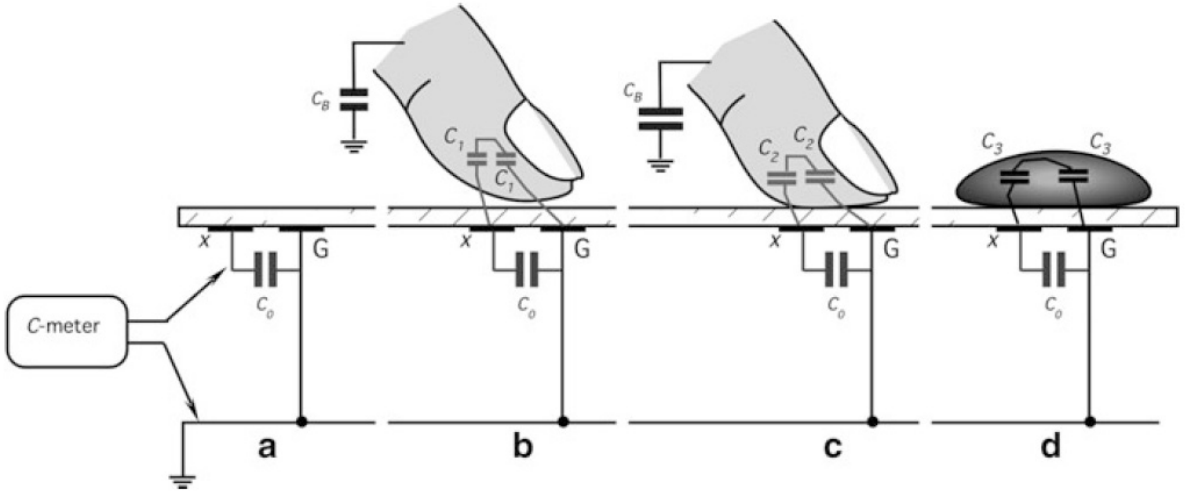

Fig. 9.14 A dual-electrode touch screen. No touch (**a**), light touch (**b**), strong touch (**c**), and a water droplet (**d**)

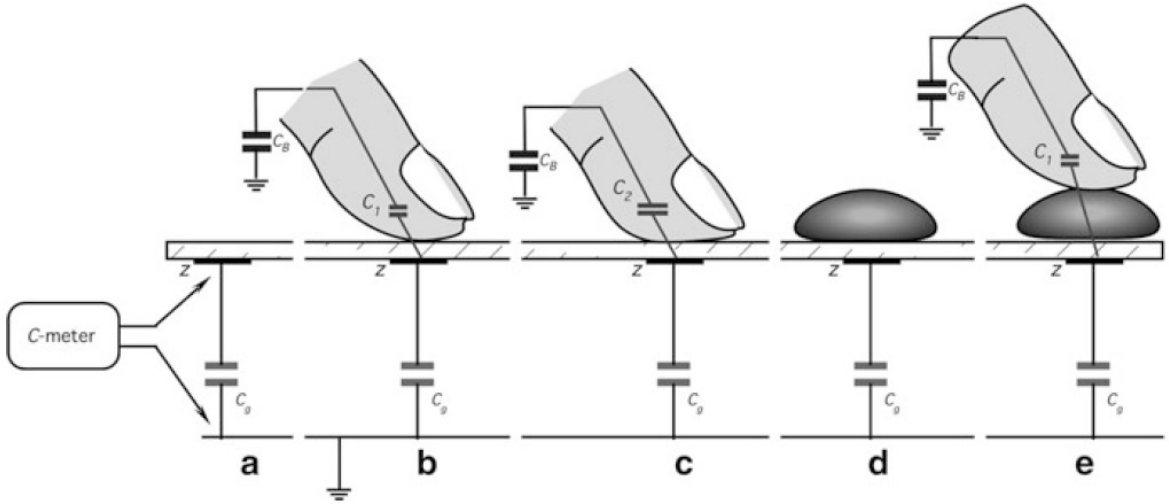

Fig. 9.15 A single-electrode touch screen. No touch (**a**), light touch (**b**), strong touch (**c**), a water droplet (**d**), and touching through a water droplet (**e**)

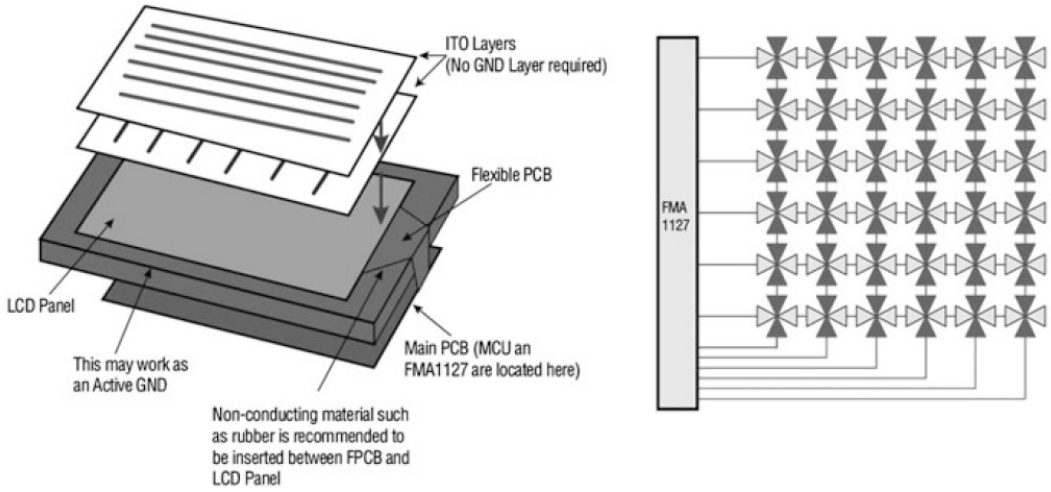

Fig. 9.16 Nongrounded touch screen for LCD panel (Courtesy of Fujitsu Microelectronics America, Inc.)

Fujitsu FMA1127 utviklingskort

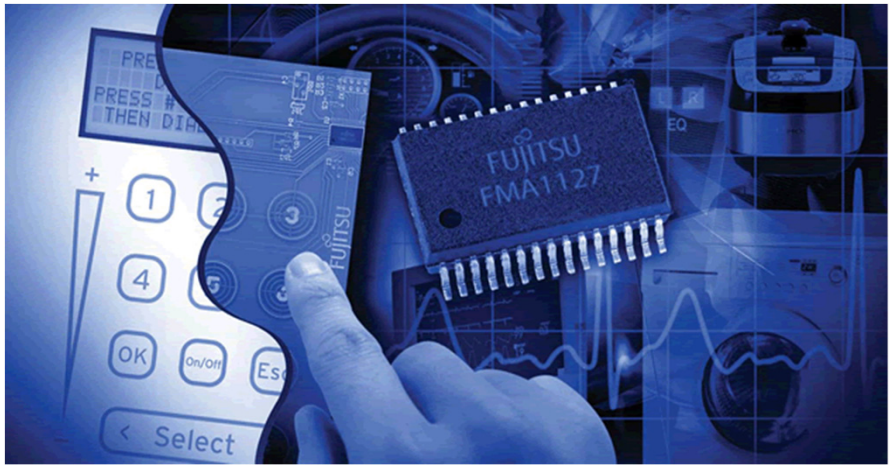

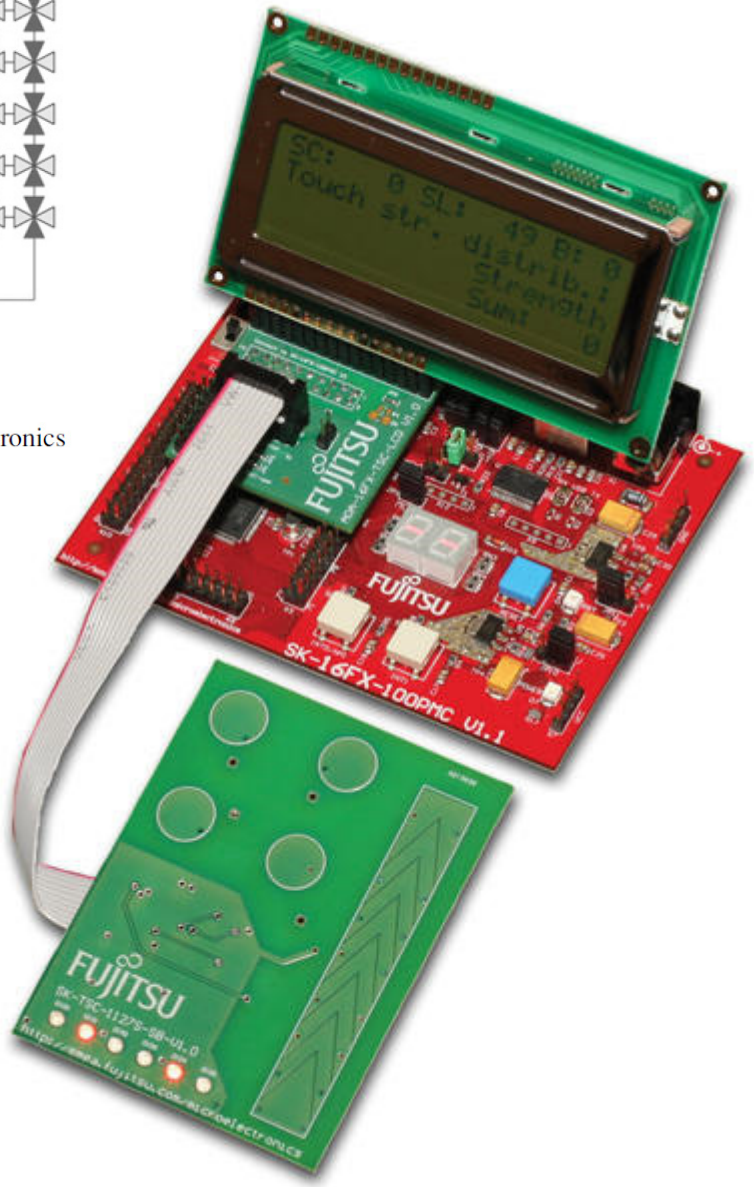

Optisk berøringsskjerm

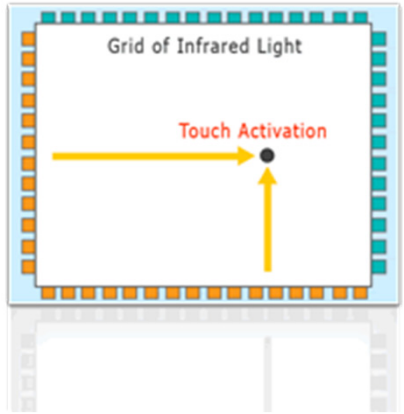

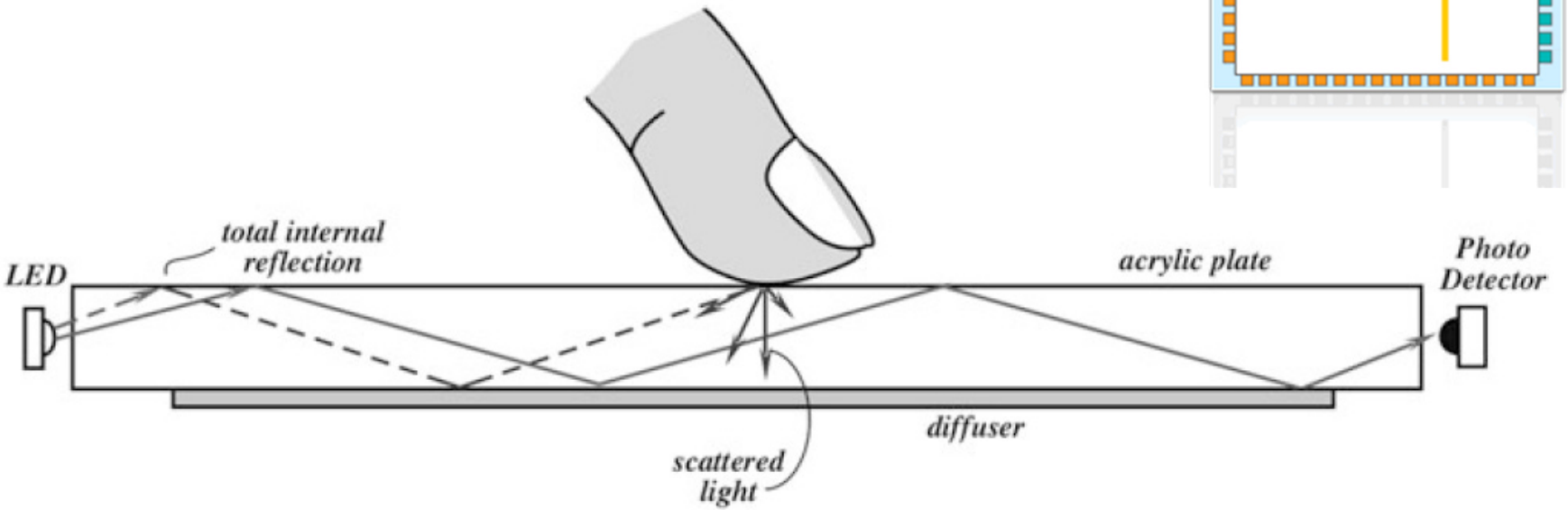

Fig. 9.17 Concept of optical touch screen

- Flere diode/detektor-par
- Dyrere enn kapsitive skjermer
- Mer følsomme for eksternt lys
- Men slipper belegg på glasset!

Electronic fingerprint sensors

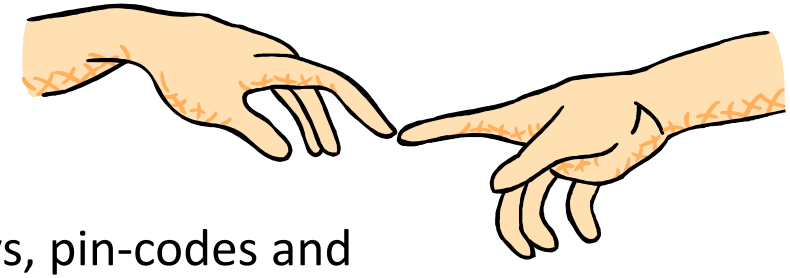

- Will eliminate the need for keys, pin-codes and access cards in a number of daily life products
- One such large-scale application will be the need for secure mobile transactions when paying for the groceries with your mobile phone at the local supermarket
- Sensors under development are based on *electrical*, *thermal*, *optical*, *pressure*, ... measurements

The Idex electrical bioimpedance based stripe sensor

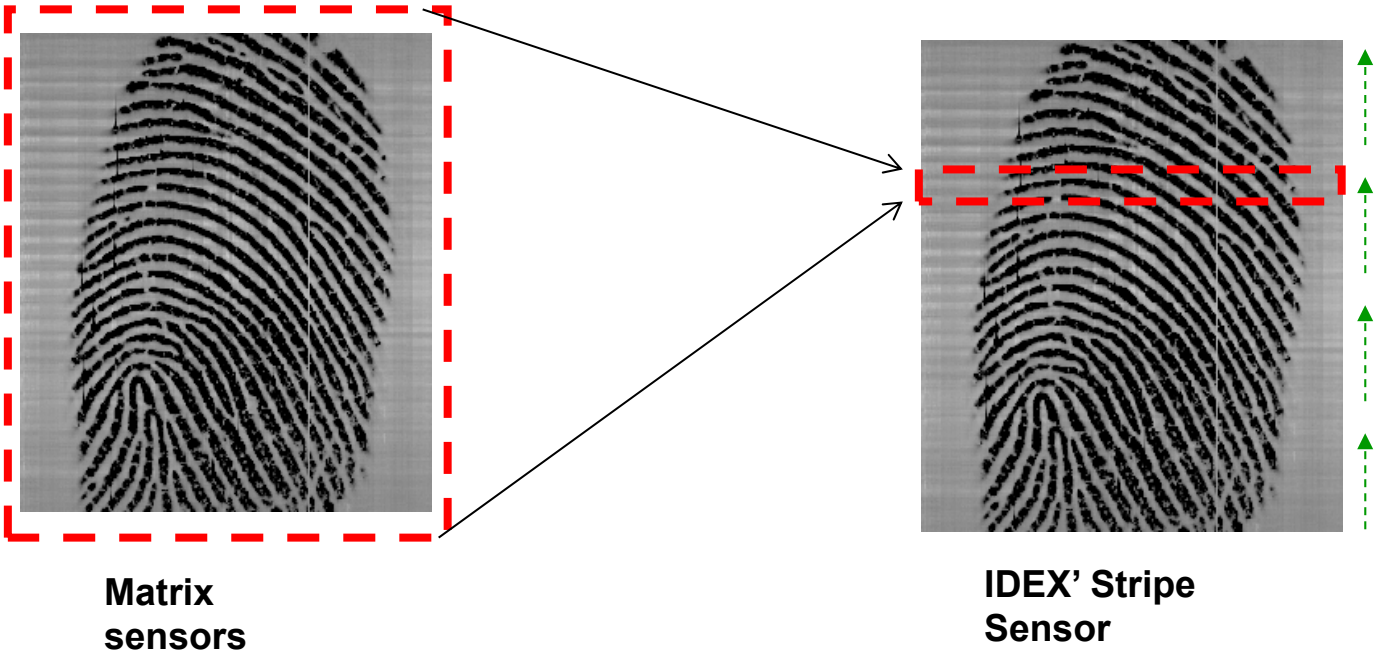

Silicon size difference = 5x

Hybrid sensor configuration

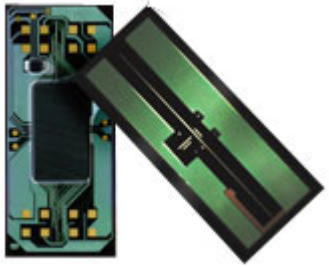

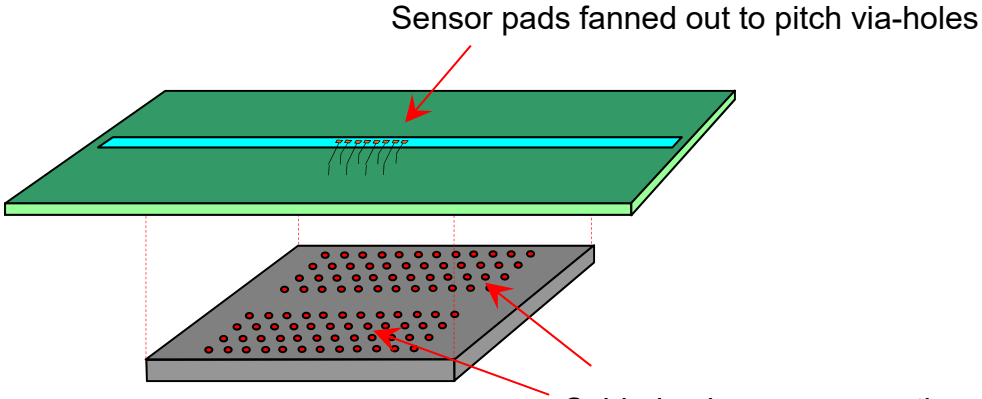

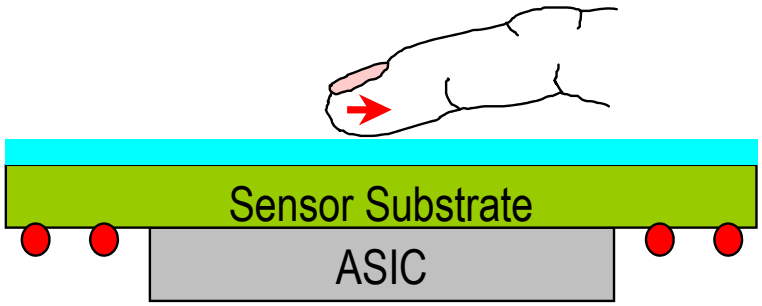

Cross-section of hybrid chip

Sensors fooled by ”gummy fingers”

- Matsumoto et al. **Proc. SPIE**, vol. 4677, 275-289, 2002
- **Nature**, 417, 583, 2002
- **Nature**, 417, 676, 2002

Idex ”gummy fingers” made from Matsumoto et al.’s recipe

- Matsumoto et al. reported that molded gelatin “gummy fingers” were able to fool about 80% of all tested fingerprint systems
- **Live finger detection** solves this problem

Live finger detection

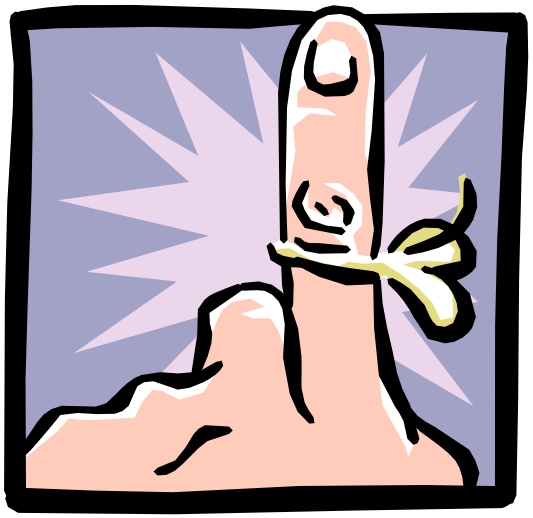

- **Solution 1:** Measure impedance (conductance, capacitance, etc.)
  Dummy: Easy to fool by applying moisture, cream or saline
  Dead finger: Dominated by stratum corneum which is already dead
- **Solution 2:** Measure temperature
  Dummy / dead finger: Easy to heat
- **Solution 3:** Measure blood oxygenation or plethysmographic pulse
  Problem: Microcirculation is cut off in cold weather
- **Solution 4:** Measure ECG pulse
  Problem: Will not work unilaterally
- **Our solution:** Bioimpedance measurements simultaneously on stratum corneum and viable skin. Dead finger will fail. Living finger with e.g. thin Latex layer will also fail

Frequency dependence

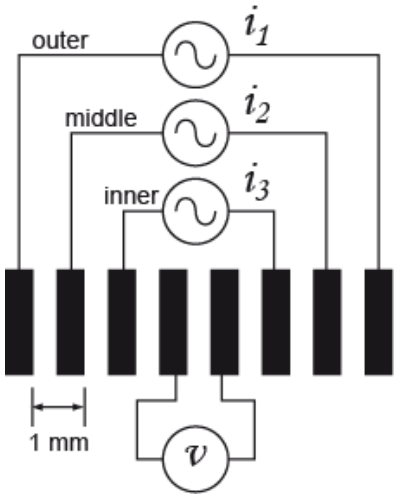

From: Yamamoto et al. Med. Biol. Eng. 14, 592-594, 1976

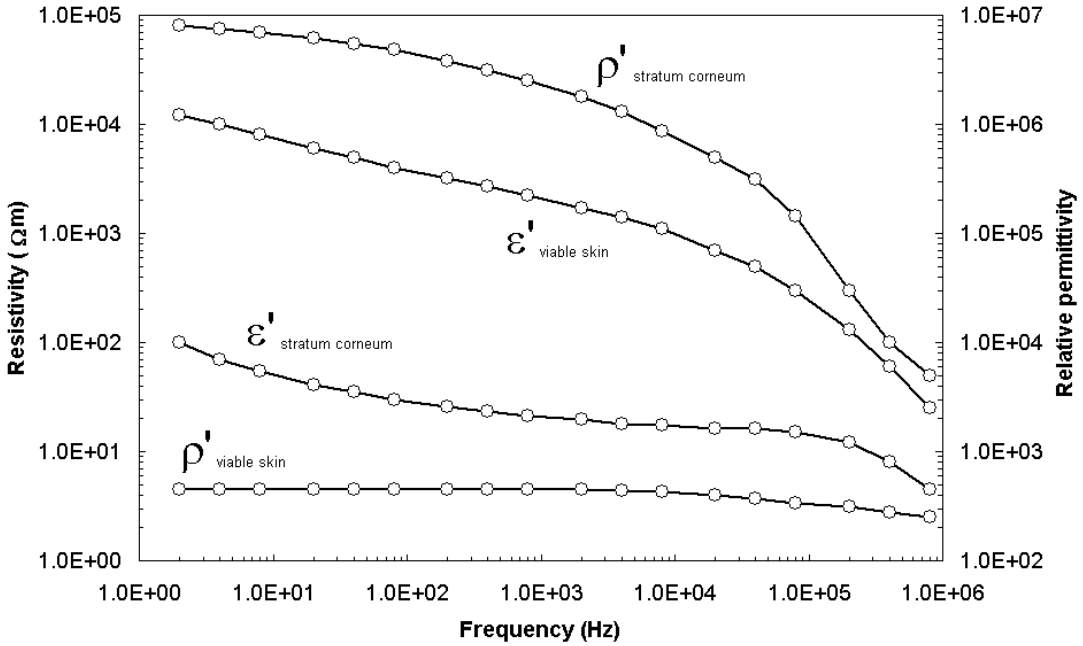

- Stratum corneum and viable skin differ e.g. in impedance levels, dispersions and anisotropy
- Electrode system optimized with regard to sensitivity distribution
- Multivariate modeling to combine measured data in a classification algorithm

Gummy- and real fingers

Measured with Solartron 1260 + 1294

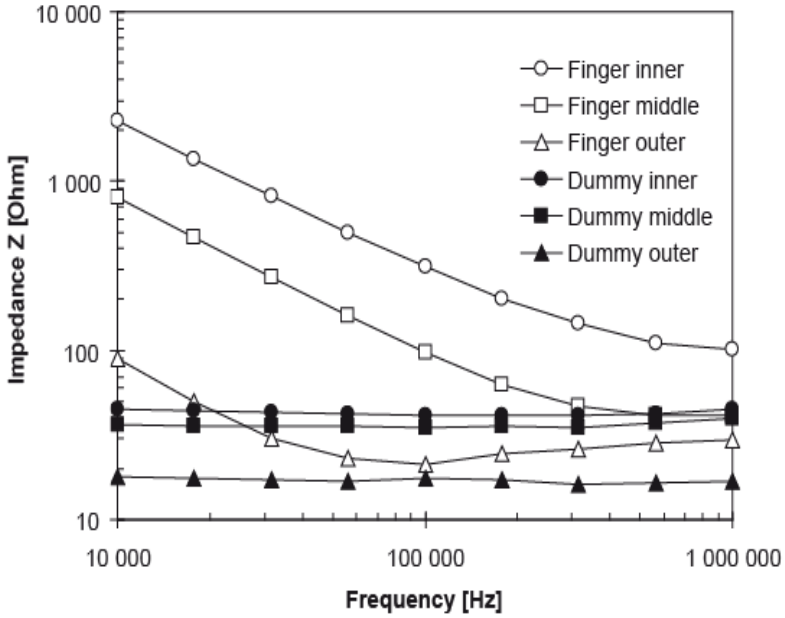

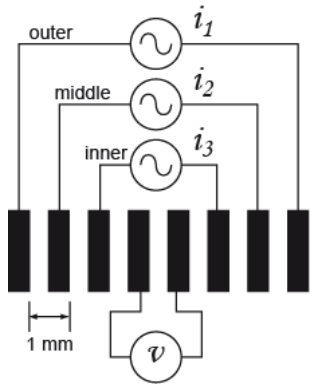

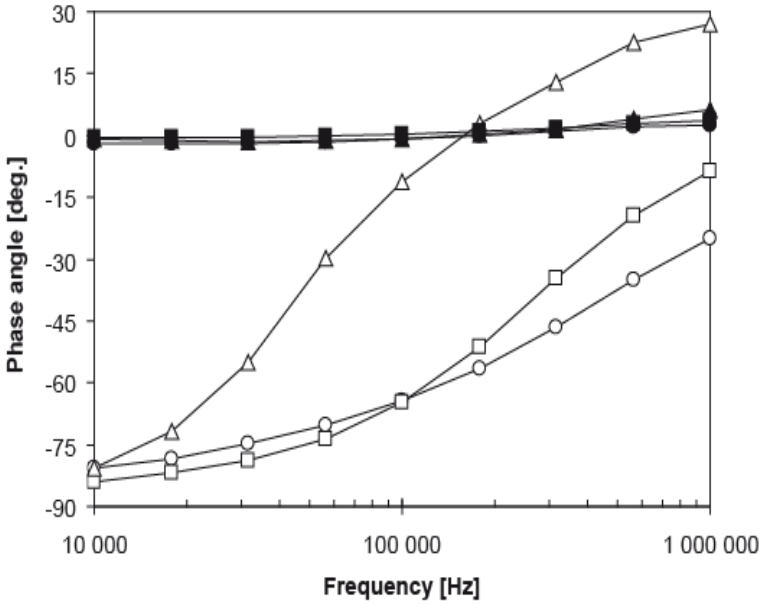

Data analysis – simple first approach

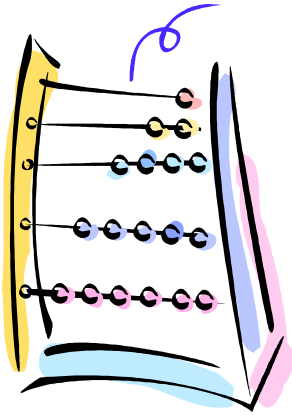

- Computed a weighted average of the three curves in the complex plane.
- This gave almost straight lines
- The lines are characterized by four numbers, e.g. the R and X of the endpoints
- Can be used as input in multivariate analysis to classify the fingers

Martinsen et al., IEEE TBME, 54, 891-894, 2007

Multivariate analysis

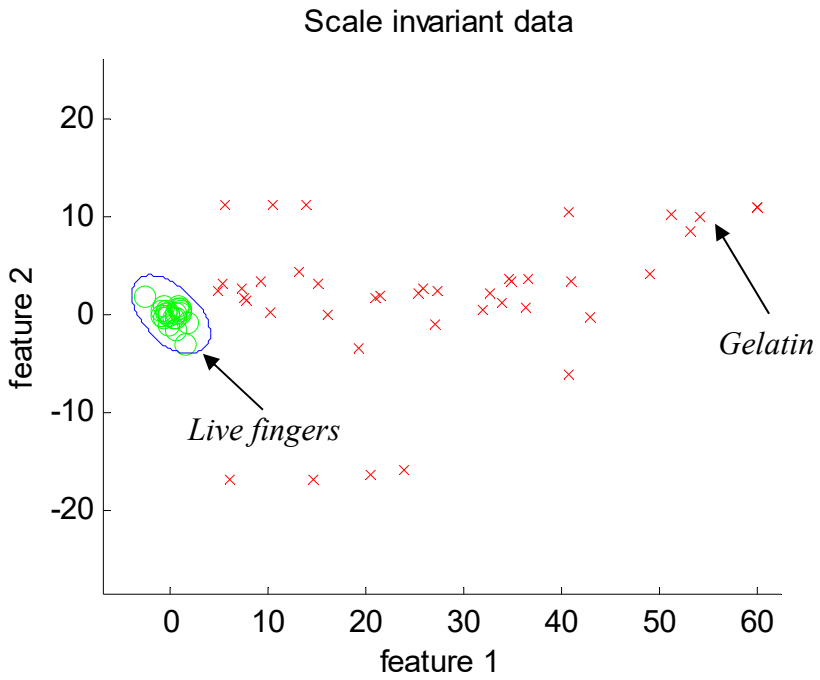

- 21 measurements on live fingers from 15 different individuals
- 41 measurements on different types of materials ranging from vegetables to gelatin fingers
- The live finger measurements (green circles) all fall within the 3σ blue ellipse (1σ = 1 standard deviation)
- All the fake materials (red crosses) are easily discriminated from the live fingers

- **Feature 1:** Slope of the line
- **Feature 2:** Reactance (X) of the center point of the line
- Using all four variables gives even better separation
- Measurement on sensor takes a few milliseconds

Pressure

$$1\text{Pa} = 1.45 \times 10^{-4}\text{lb/in}^2 = 9.869 \times 10^{-6}\text{atm.} = 7.5 \times 10^{-4}\text{cmHg}$$

- 1 Pa = 1 N/m^2
- 1 Torr = 1 mm Hg (Blodtrykk 120/70)

Kvikksølvbarometer

- Kvikksølvet kortslutter motstandstråden
- Bruker Wheatstone bridge
- Høye krav til nivåbestemmelse
- Stort og sårbart
- Kvikksølvdamp

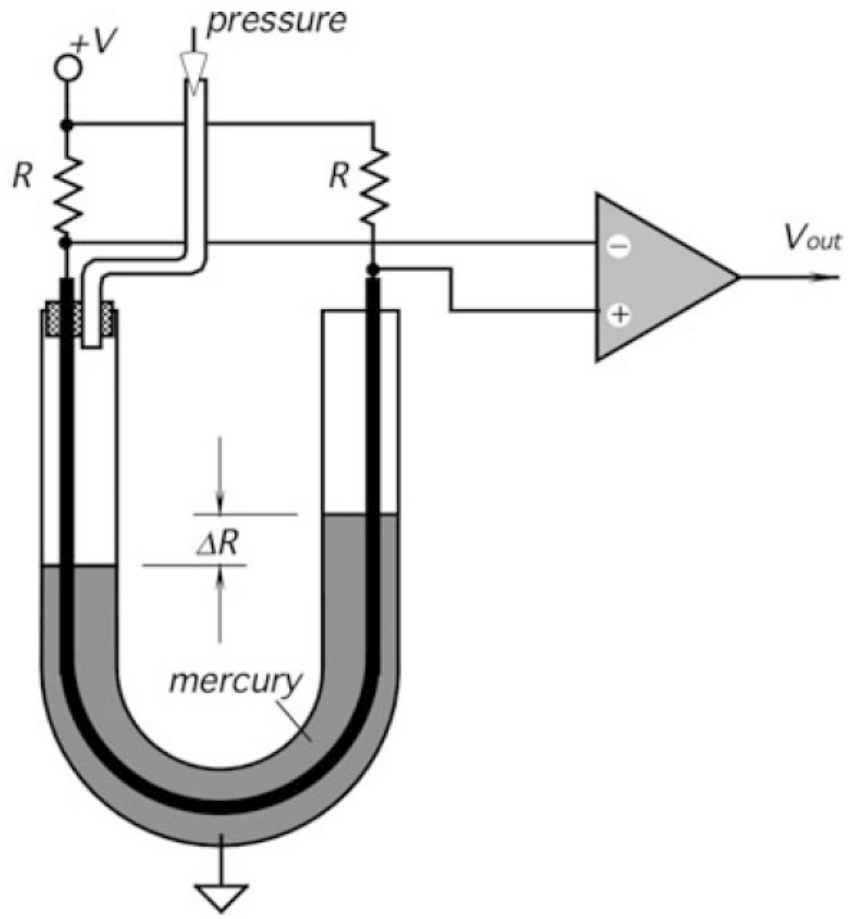

Fig. 10.1 Mercury-filled, U-shaped sensor for measuring gas pressure

Membraner og plater

- I dag er Si-membraner vanligst
- Hvis ikke radius > 100 ggr tykkelsen → tynn plate (og ikke membran)
- Maks utslag på plata:

$$z_{max} = \frac{3(1-v^2)r^4 p}{16Eg^3}$$

E = Young's modul

v = Poisson's ratio

r = radius

g = tykkelse

p = trykkforskjell

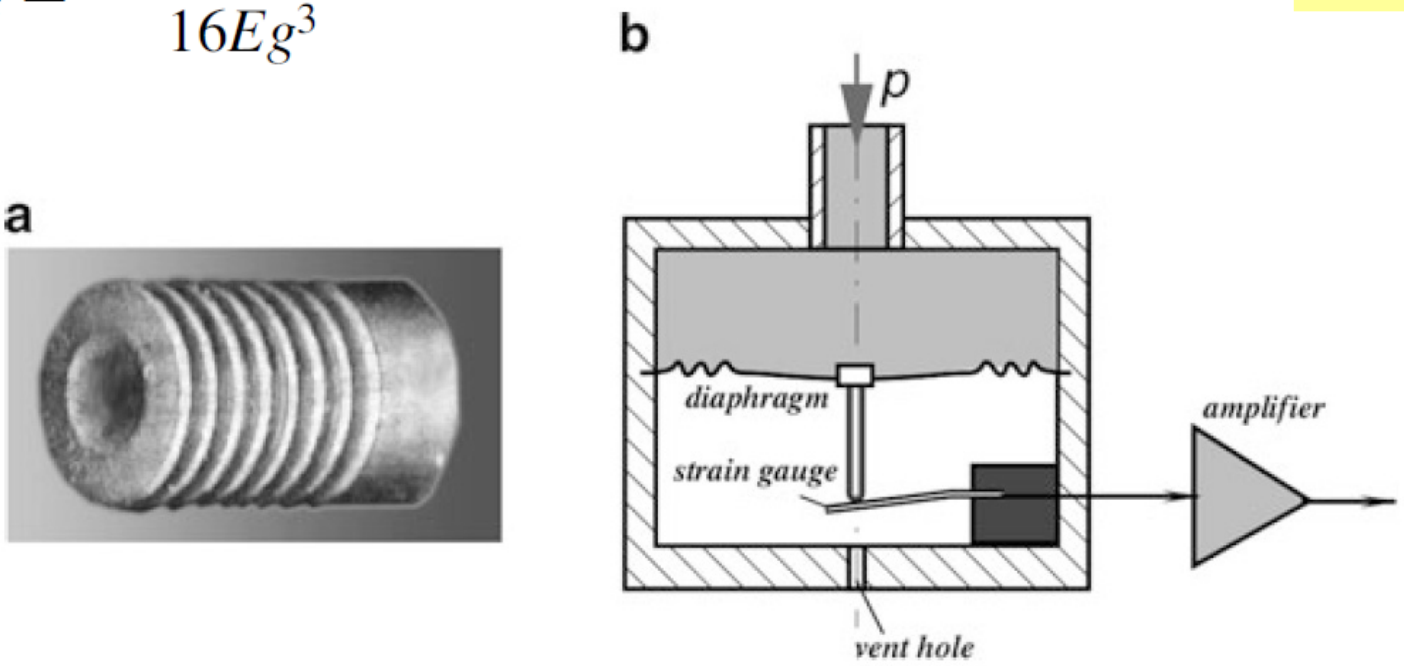

Fig. 10.2 Steel bellows for a pressure transducer (**a**) and metal corrugated diaphragm for the conversion of pressure into linear deflection (**b**)

Piezoresistiv sensor

- Piezoresistivt element (strekklapp)
- Nesten som en mekanisk Hall-sensor
- 1 mm^2 stort silisium-membran

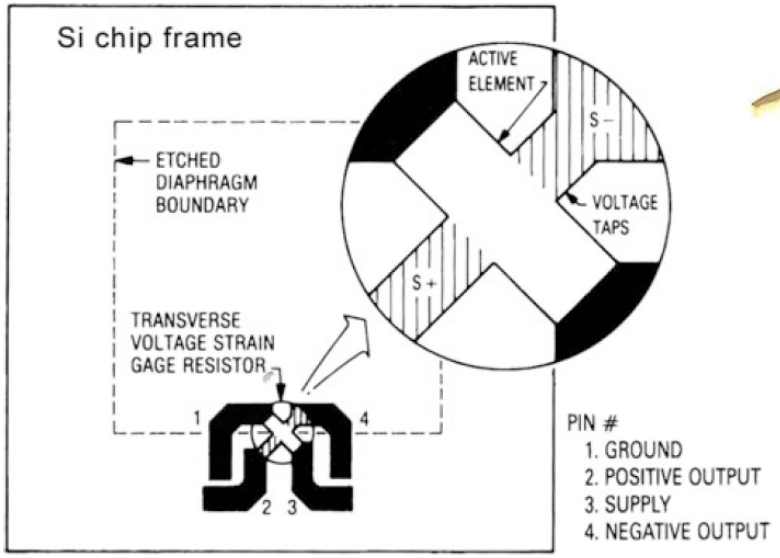

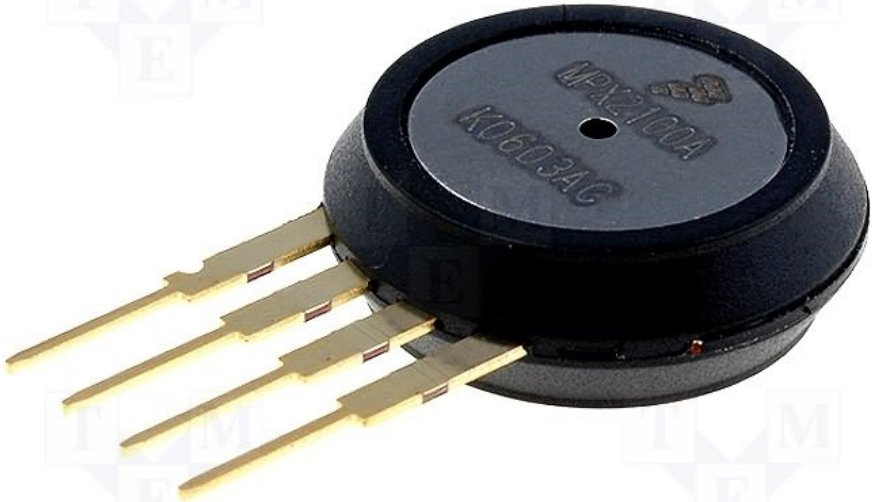

Fig. 10.5 Basic uncompensated piezoresistive element of Motorola MPX pressure sensor (Copyright of Motorola, Inc. Used with permission)

Variable Reluctance Pressure (VPR) sensor

- Bruker et membran med høy magnetisk permeabilitet (mymetall)
- Luft har mye høyere magnetisk resistans og bestemmer derfor fluksen (og induktansen)
- Bevegelse på ca 25 – 30 µm

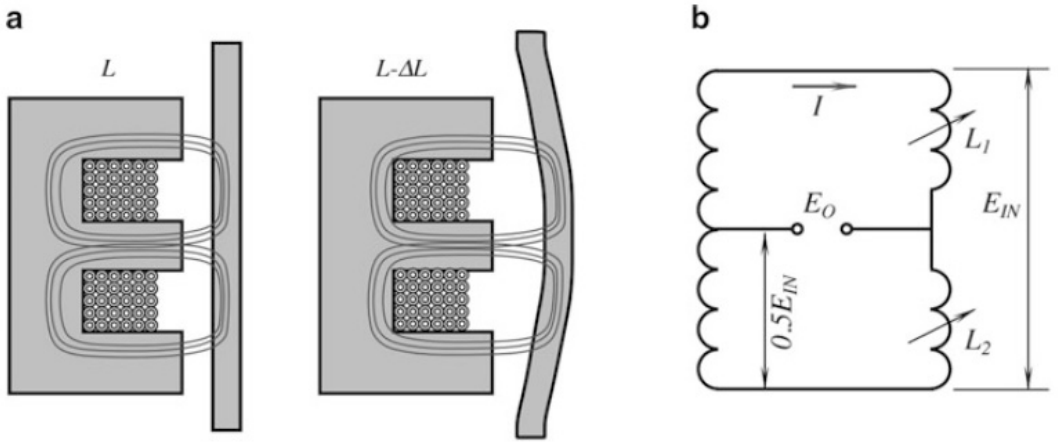

Fig. 10.12 Variable-reluctance pressure sensor. Basic principle of operation (**a**) and equivalent circuit (**b**)

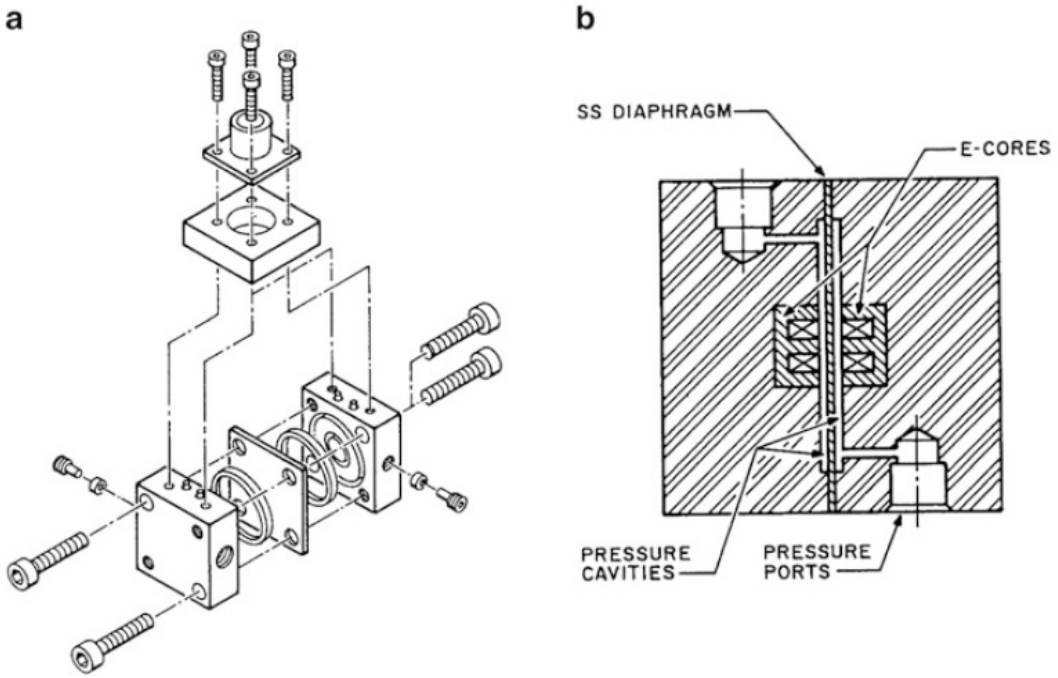

Fig. 10.13 Construction of a VRP sensor for low-pressure measurements. Assembly of the sensor (**a**) and double E-core at both sides of the cavity (**b**)

Pirani vacuum-måler

- NTC termistorer som varmekilder
- Selvbalanserende bro gir konstant T_r
- Hvis de kjøles (pga konveksjon) like mye gir broa ut null
- Kjøles bedre jo høyere trykket er
- Både positiv og negativ feedback til opampen
- C hindrer oscillasjon

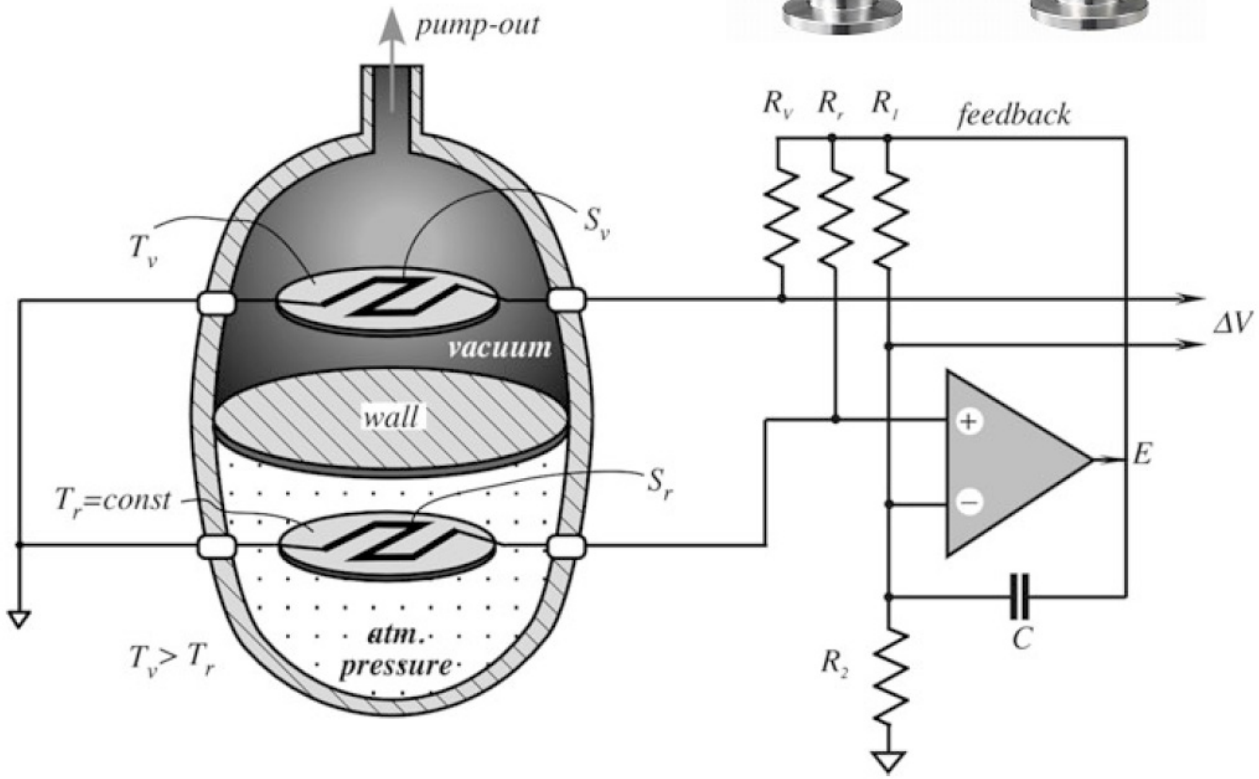

Fig. 10.17 Pirani vacuum gauge with NTC thermistors operating in self-heating mode

Strømnings-sensorer

$$\Lambda = \frac{V}{\Delta t} = \int \frac{\Delta x}{\Delta t} dA = \int v dA$$

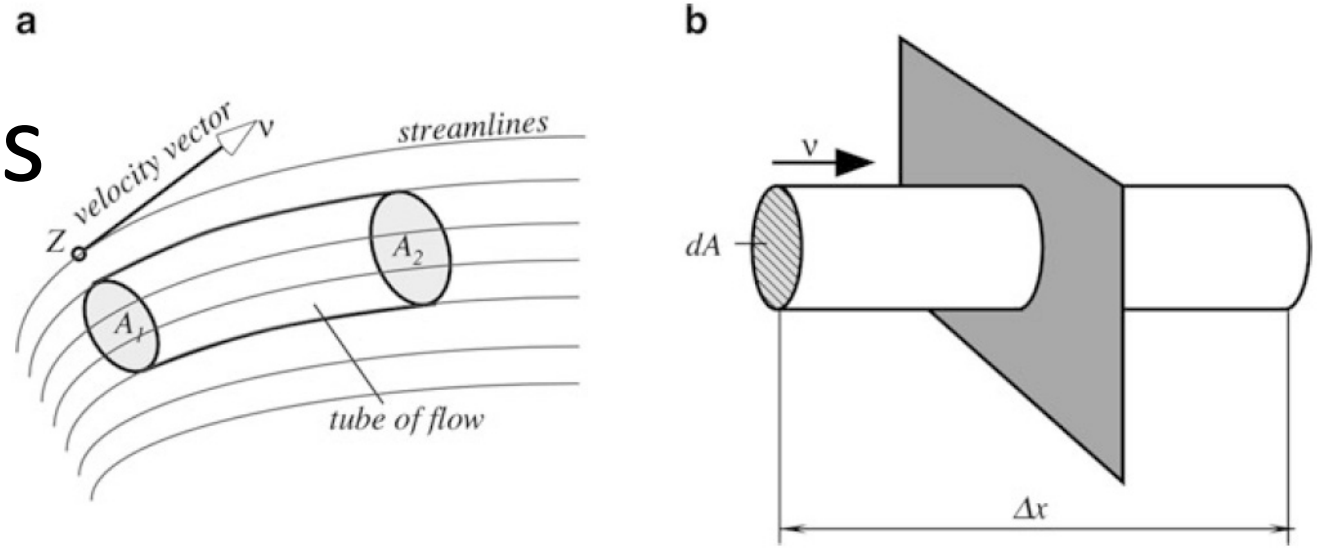

Fig. 11.1 Tube of flow (**a**) and flow of a medium through a plane (**b**)

$$\frac{dM}{dt} = \rho A \bar{v}$$

Fig. 11.2 Profile of velocity of flow in a pipe

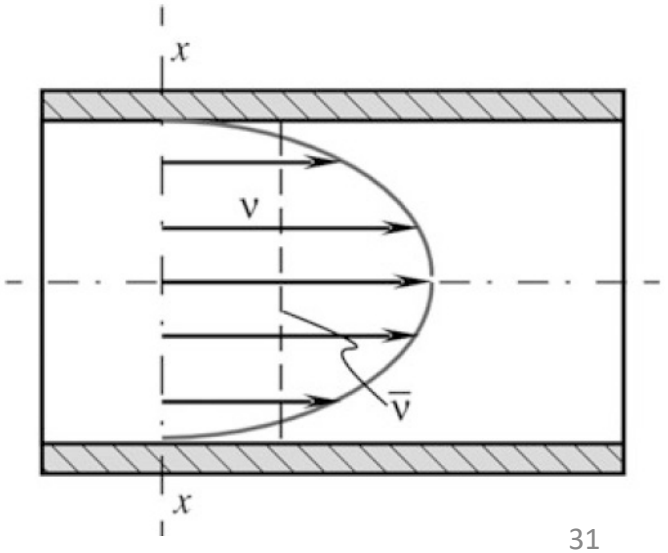

- Ønsker å vite masse/tid eller volum/tid

Trykkgradient-metoden

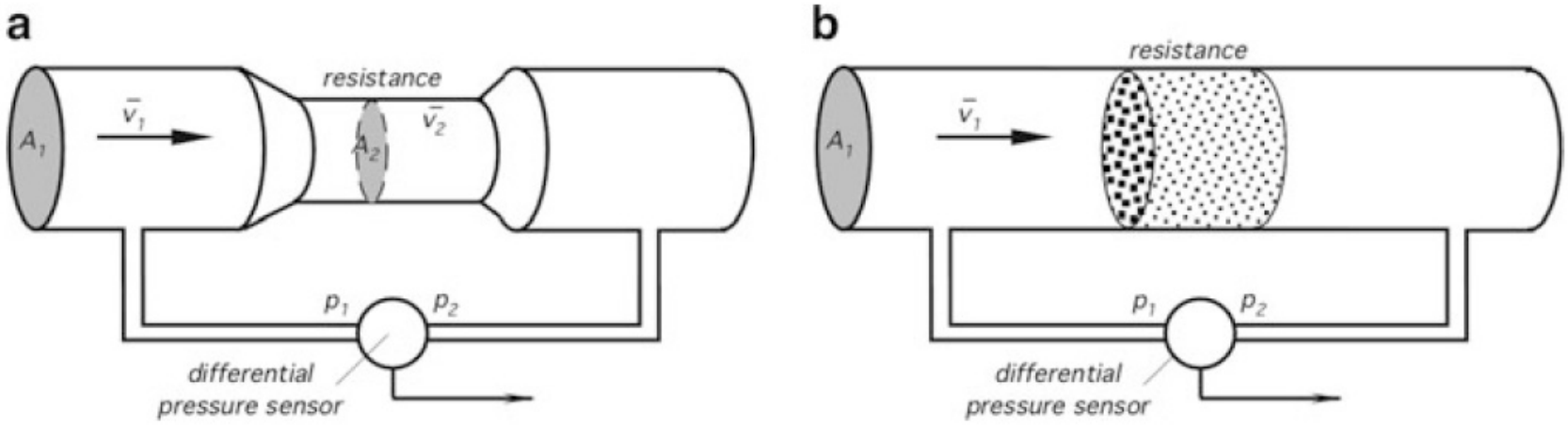

Fig. 11.3 Two types of flow resistors: a narrow channel (**a**) and a porous plug (**b**)

- Bernoulli-likningen (1738):
  Fra trykk til strømningshastighet

$$p + \rho\left(\frac{1}{2}v_a^2 + gy\right) = const$$

- Oppløsning på ca. 14-15 bit.
  Nøyaktighet på ca. 9-10 bit

Dielektrikum for å hindre kortslutning

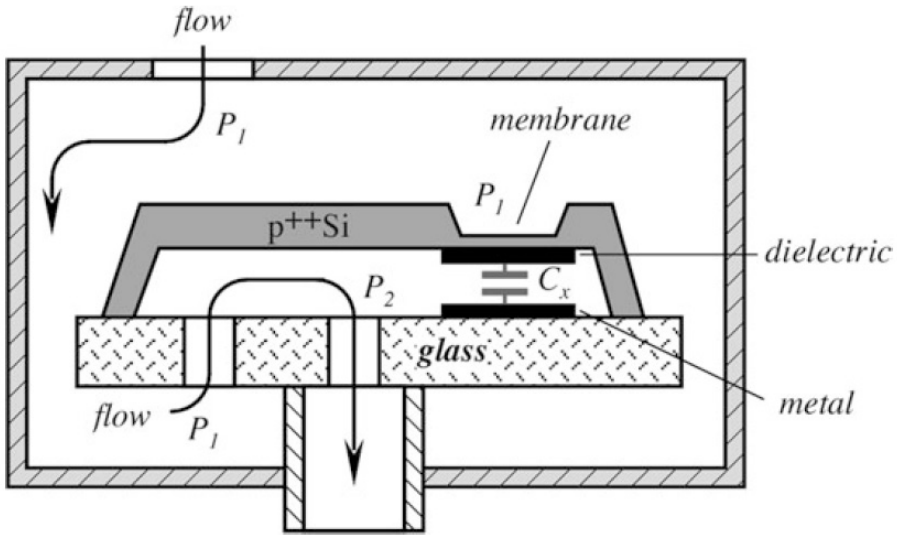

Fig. 11.4 Structure of a gas microflow sensor utilizing capacitive pressure sensor

Termo-anemometre

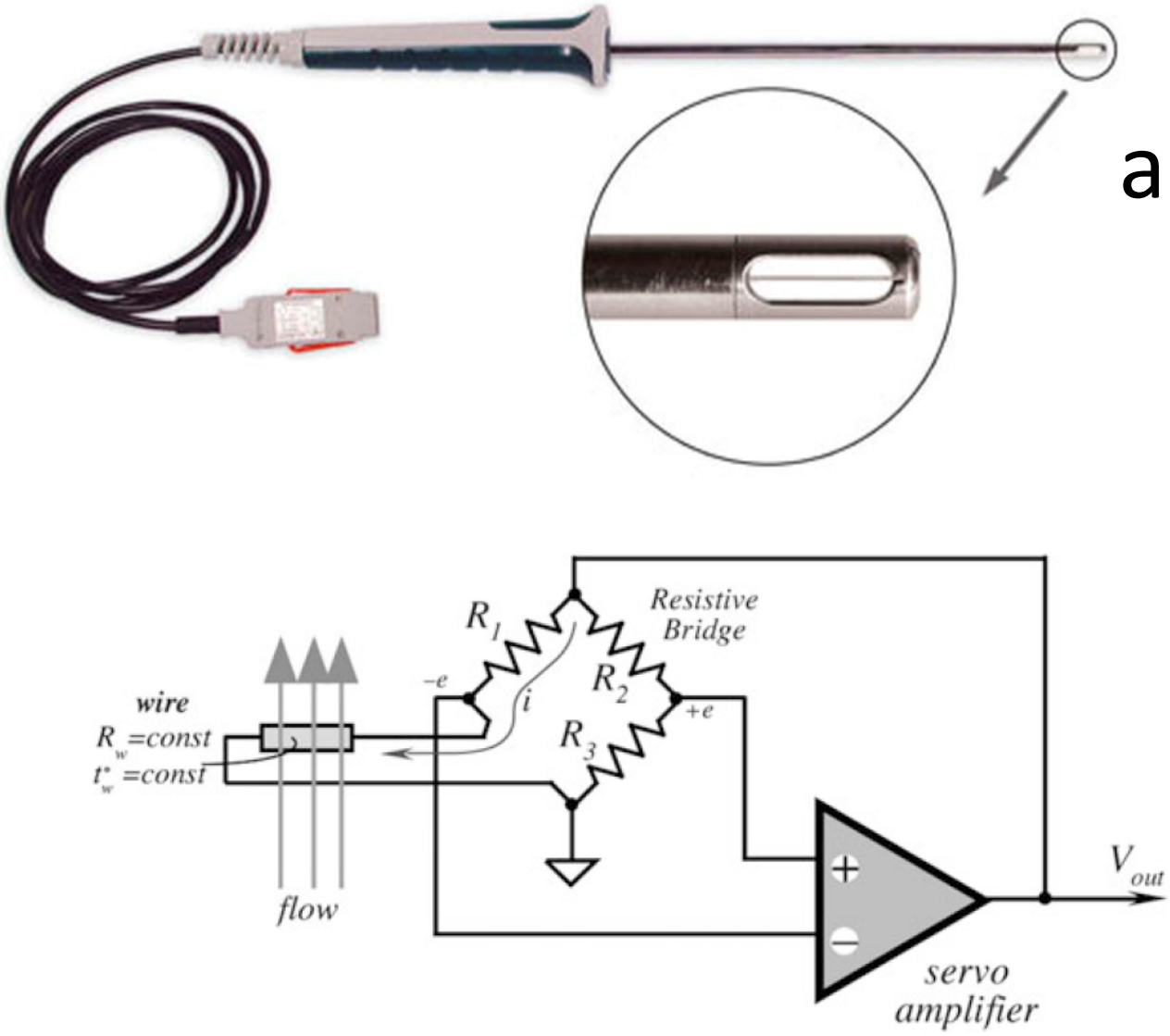

Fig. 11.5 Null-balanced bridge for a constant temperature hot-wire anemometer

- Dupp, farge, radioaktivt stoff eller varme
- Opptil ca. 60 m/s
- Konstant spenning eller konstant temperatur
- Wolfram har høy temp koeff men ikke inert
- Platina er mer inert men lite robust
- Platina-iridium brukes men wolfram mest populært

Wire vs. film

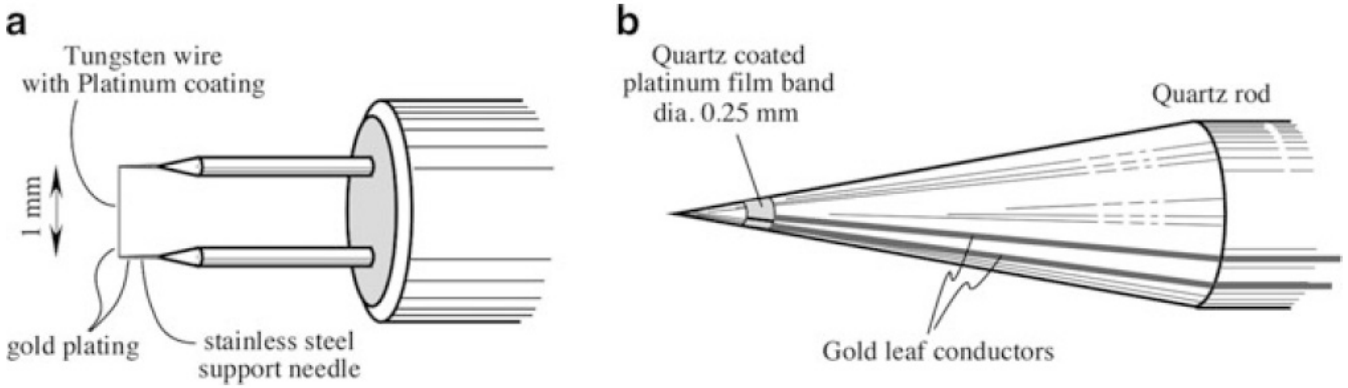

Fig. 11.6 Hot-wire probe (**a**) and a conical hot-film probe (**b**)

Film er bedre fordi:

- Better frequency response (when electronically controlled) than a hot wire of the same diameter because the sensitive part of the film sensor has a larger surface area
- Lower heat conduction to the supports for a given length to diameter ratio due to the low thermal conductivity of the substrate material. A shorter sensing length can thus be used
- More flexibility in sensor configuration. Wedge, conical, parabolic, and flat surface shapes are available
- Less susceptible to fouling and easier to clean. A thin quartz coating on the surface resists accumulation of foreign material

Pulsbreddemodulator

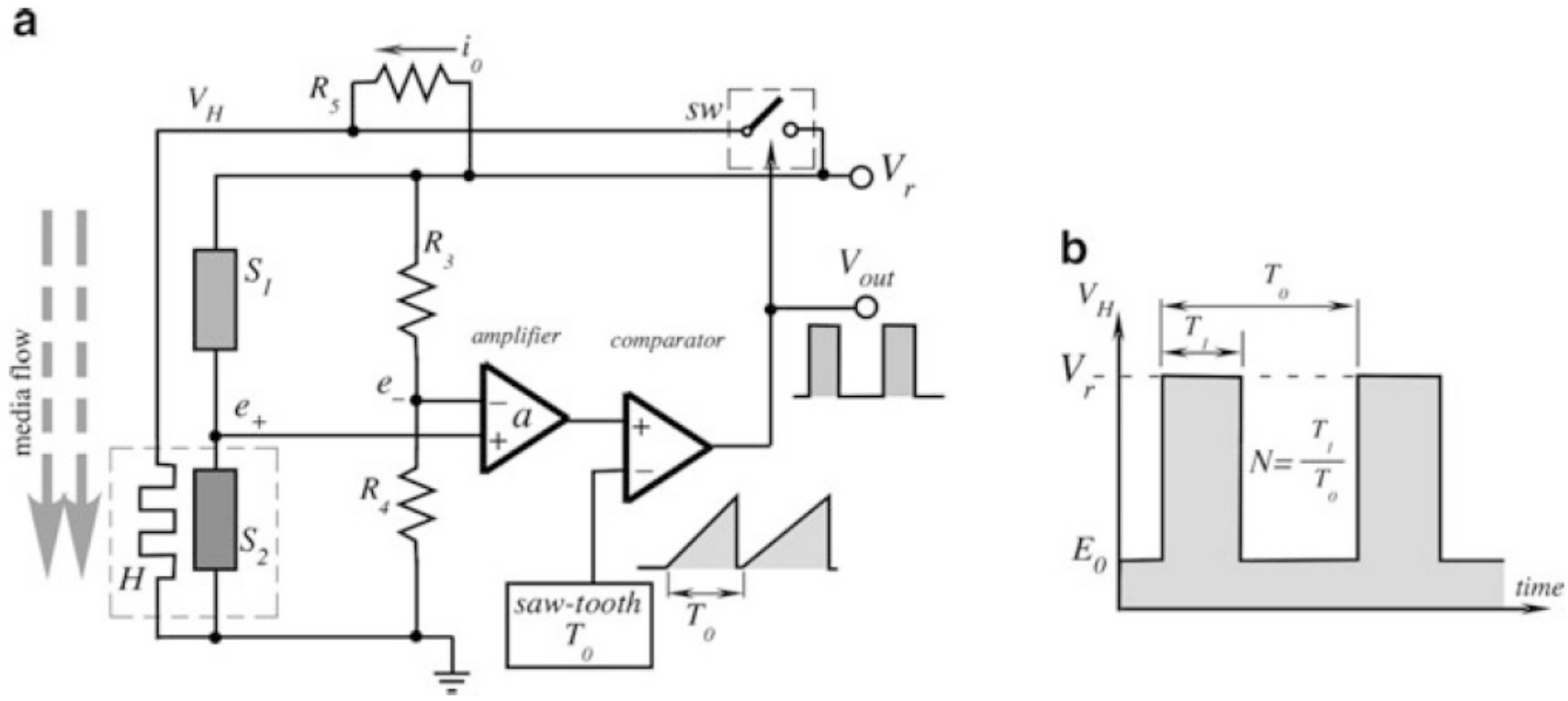

Fig. 11.10 Control circuit of a thermoanemometer with PWM modulator (**a**); transfer function for the r.m.s. of PWM signal (**b**)

- Bredere pulser → mer varme genereres
- i_0 er for å kompensere for varmeledning til resten av sensorstrukturen

Gass-sensor

- Titan-filmer er både varmeelement og temperatursensorer

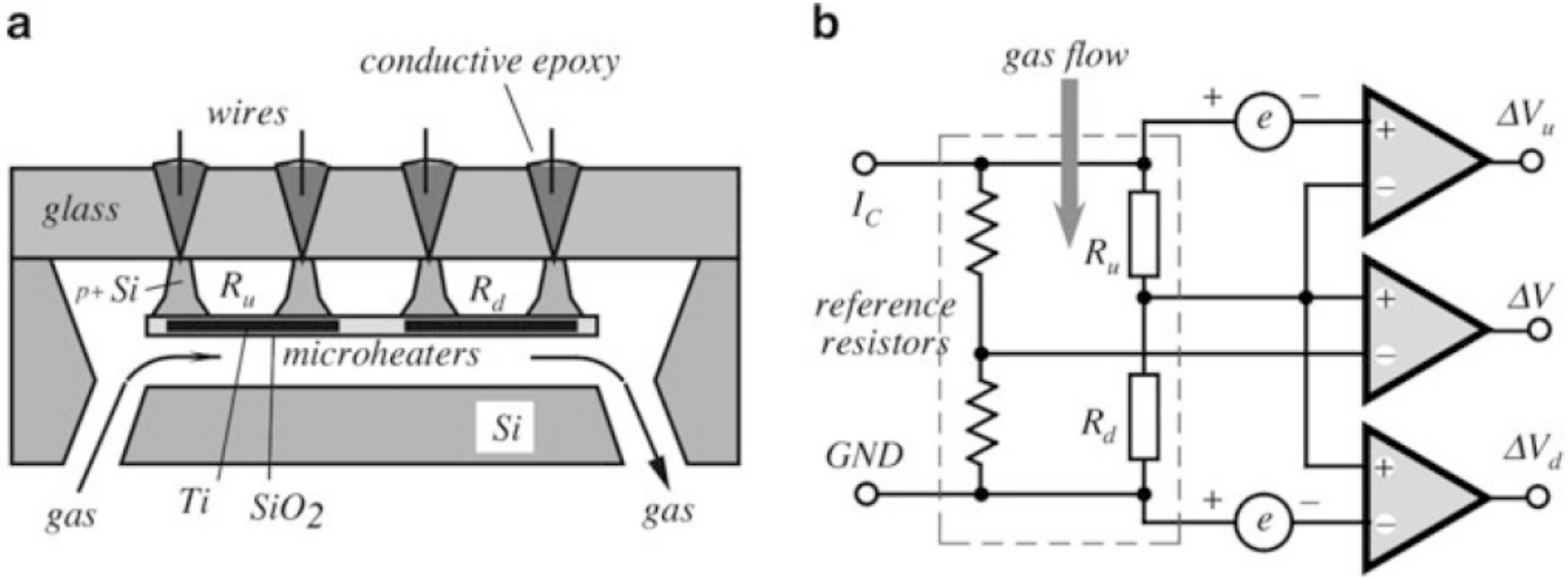

Fig. 11.12 Gas microflow sensor with self-heating titanium resistors sensor design (**a**); interface circuit (**b**). R_u and R_d are resistances of the up- and downstream heaters respectively (adapted from [10])

Ultralyd (Doppler)

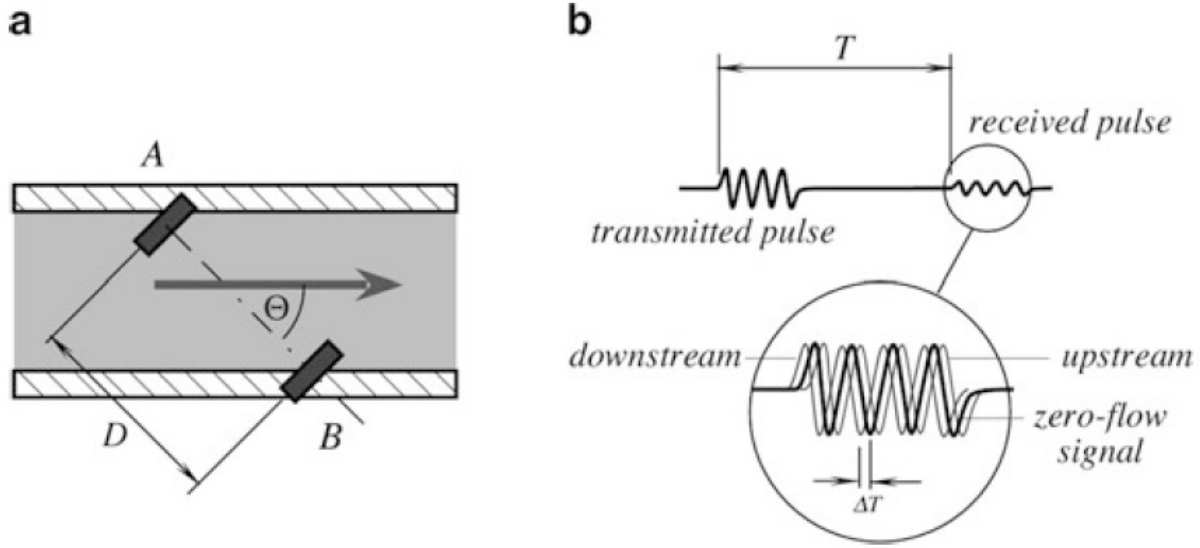

Fig. 11.13 Ultrasonic flowmeter position of transmitter–receiver crystals in the flow (**a**); waveforms in the circuit (**b**)

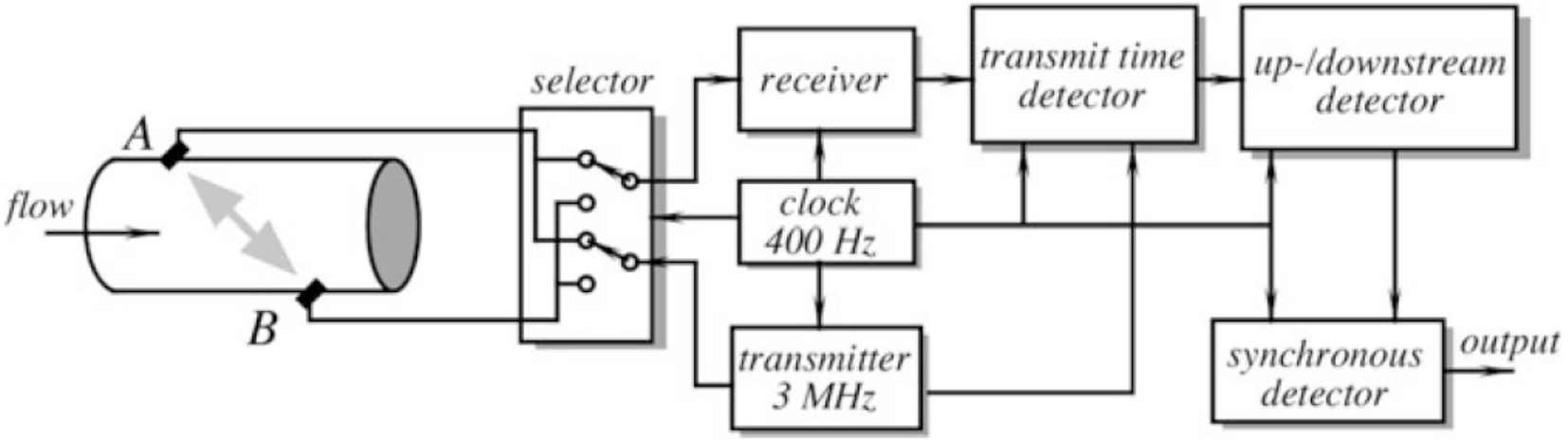

Fig. 11.14 Block diagram of an ultrasonic flowmeter with alternating transmitter and receiver

Elektromagnetisk sensor

- Målt spenning: $V = \frac{2\Lambda B}{\pi a}$

Eksiterer med AC magnetfelt
Jfr. firelektrodemåling

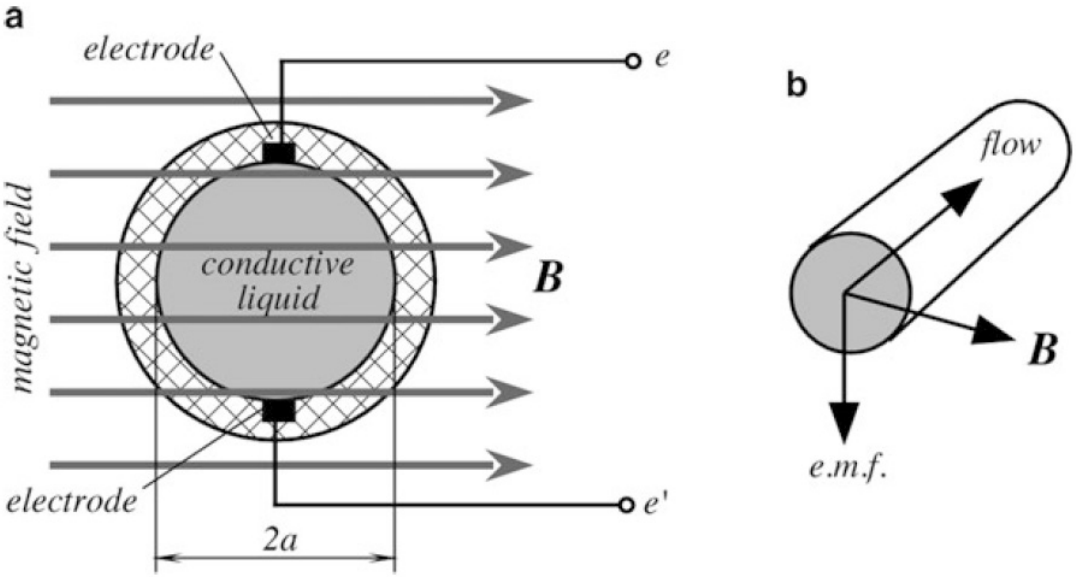

Fig. 11.16 Principle of electromagnetic flowmeter position of electrodes is perpendicular to the magnetic field (**a**); relationships between flow and electrical and magnetic vectors (**b**)

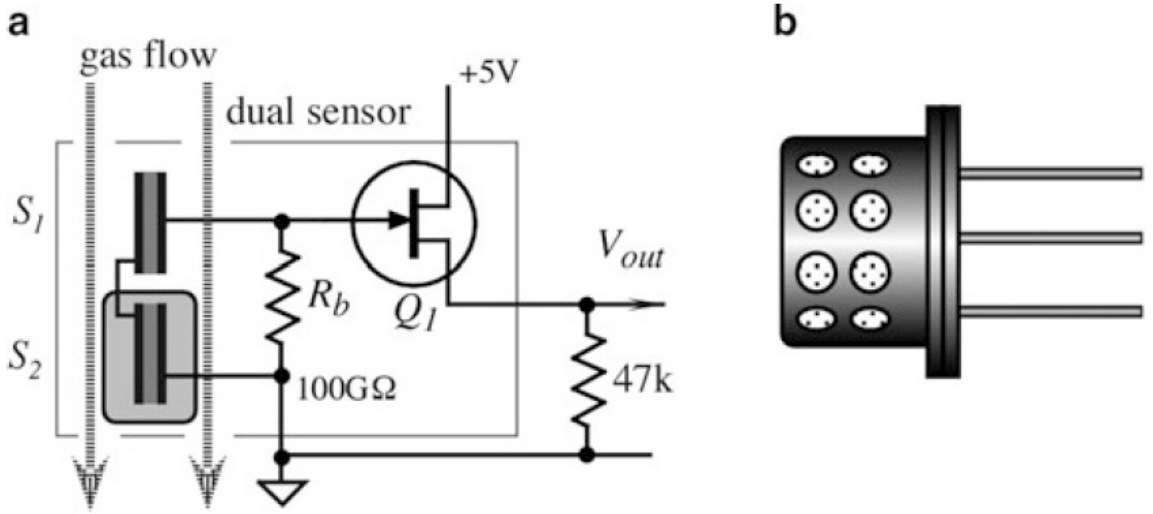

Breeze sensor

Måler strømning
eller ikke strømning

Fig. 11.18 Piezoelectric breeze sensor circuit diagram (**a**); packaging in a TO-5 can (**b**)

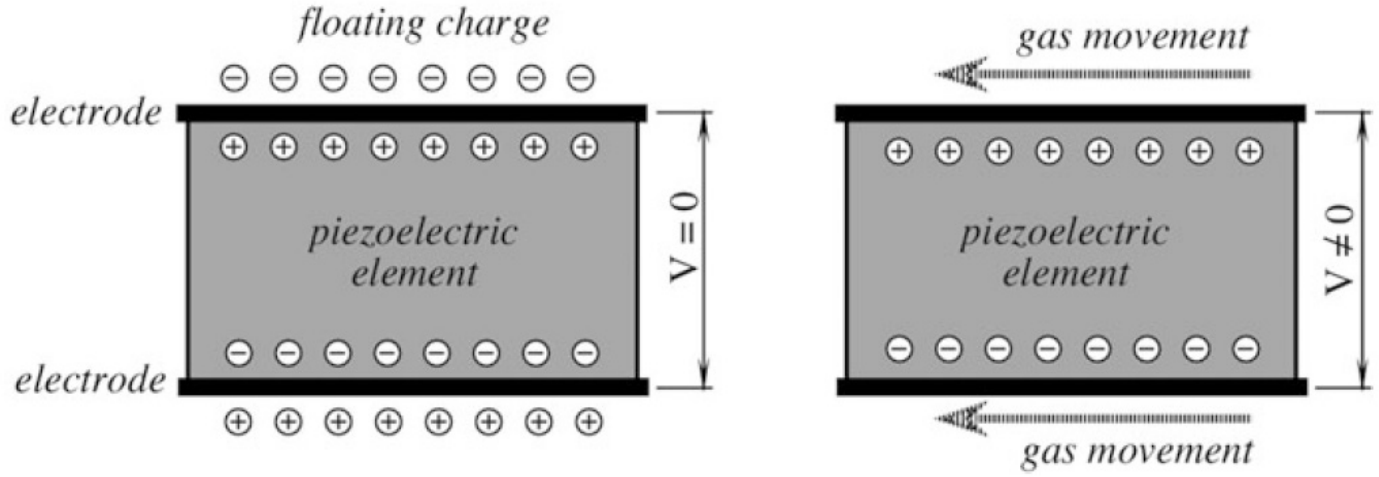

Fig. 11.19 In a breeze sensor, gas movement strips off electric charges from the surface of a piezoelectric element

Coriolis-sensor

- Noe som allerede beveger seg bringes inn i en ny referanseramme med en annen bevegelse.
- Corioliskraften er produktet av massen, rotasjonsfrekvensen og midlere hastighetsvektor til massen som beveger seg

$$\boldsymbol{F} = 2m\omega\boldsymbol{v}$$

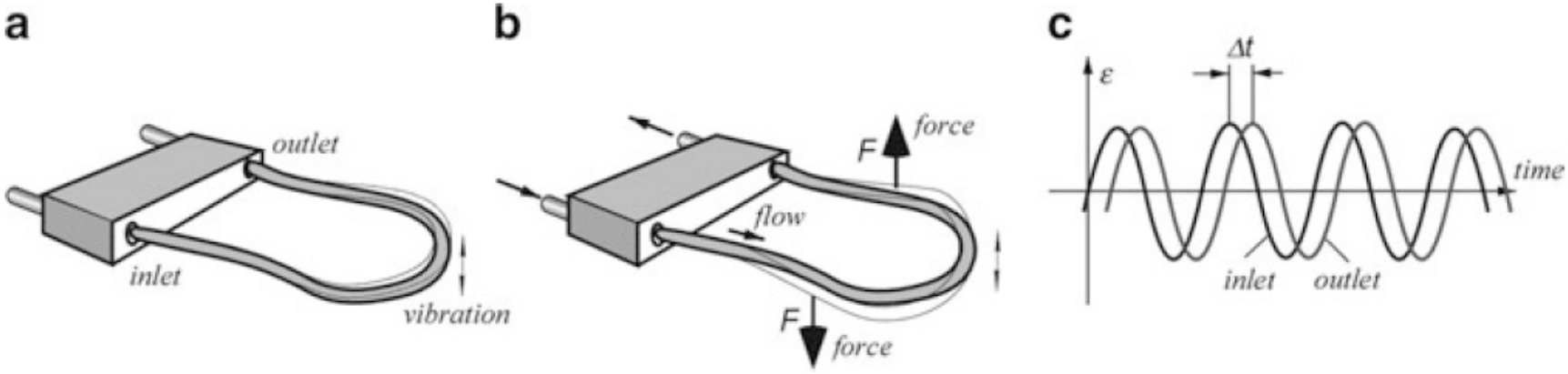

Fig. 11.20 Coriolis tube with no flow (**a**); twist of the tube with flow (**b**); vibrating phase shift resulted from Coriolis forces (**c**)

Drag force sensor

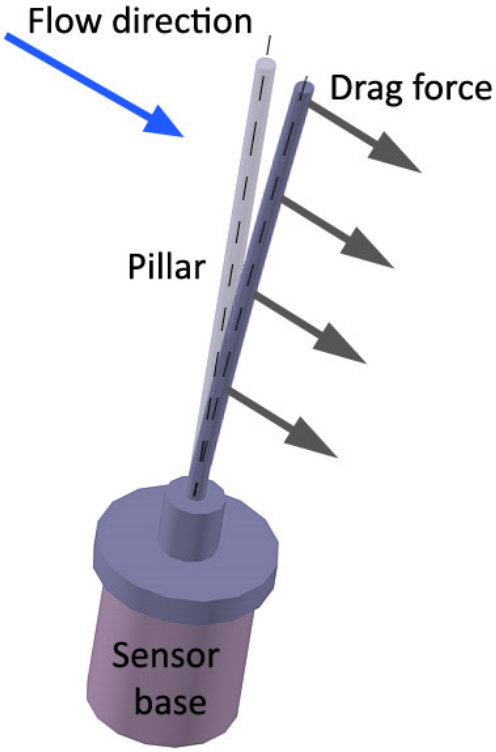

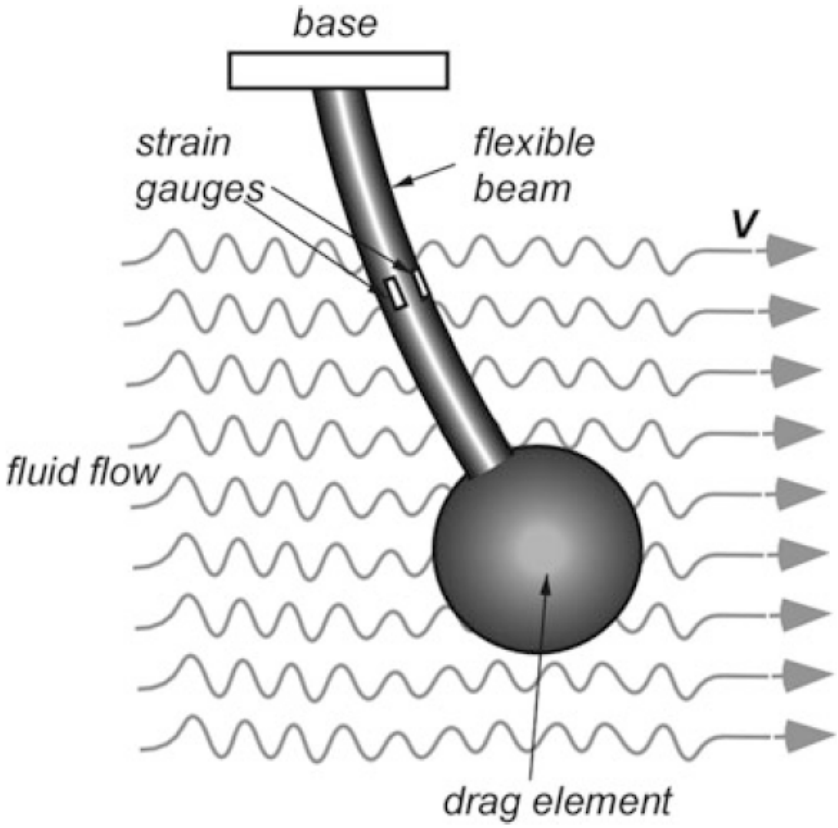

Ioniserende røykvarsler

ioniserer luftmolekylene
til ioner og elektroner

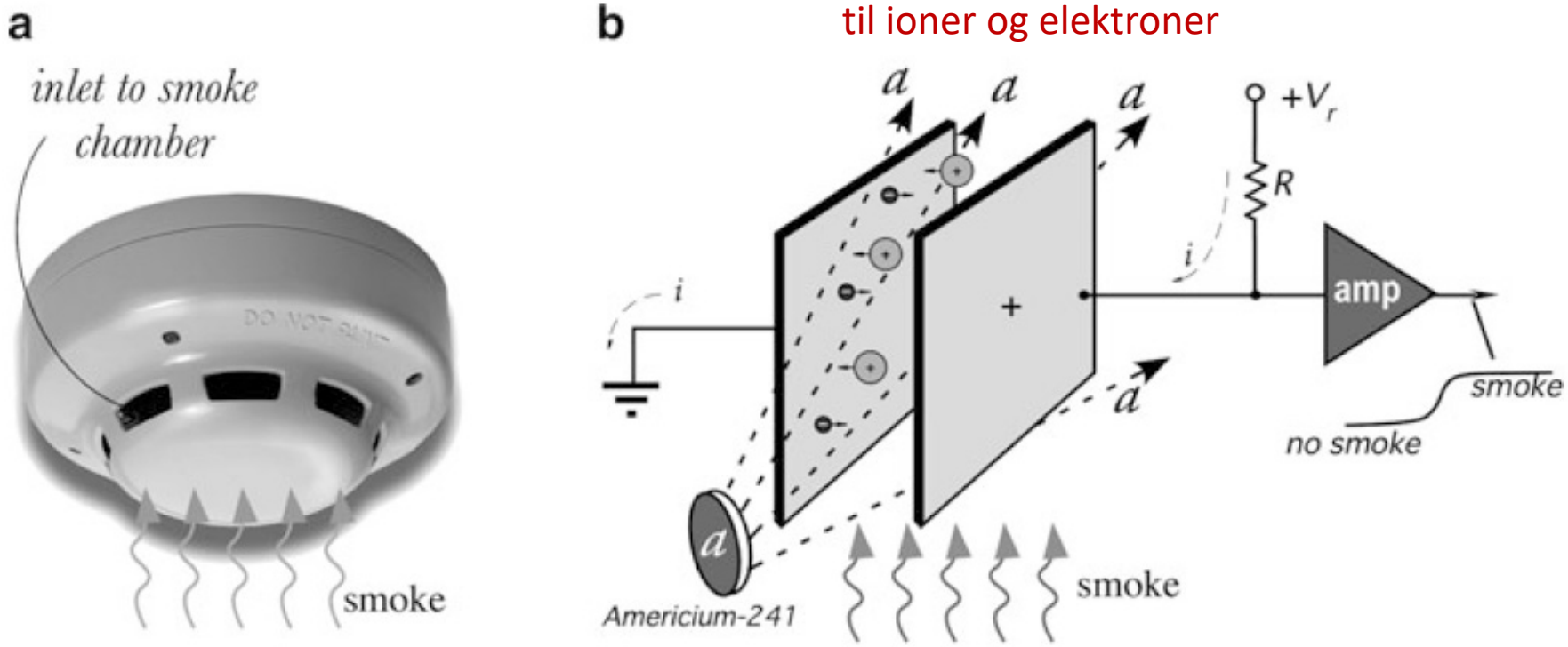

Fig. 11.22 Smoke detector (**a**) and a concept of the ionization smoke sensor (**b**)

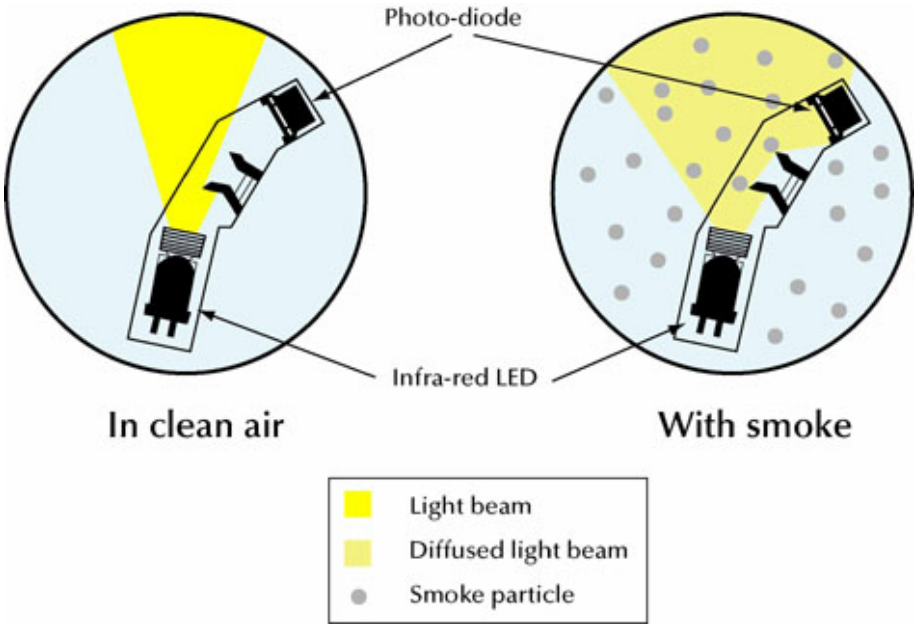

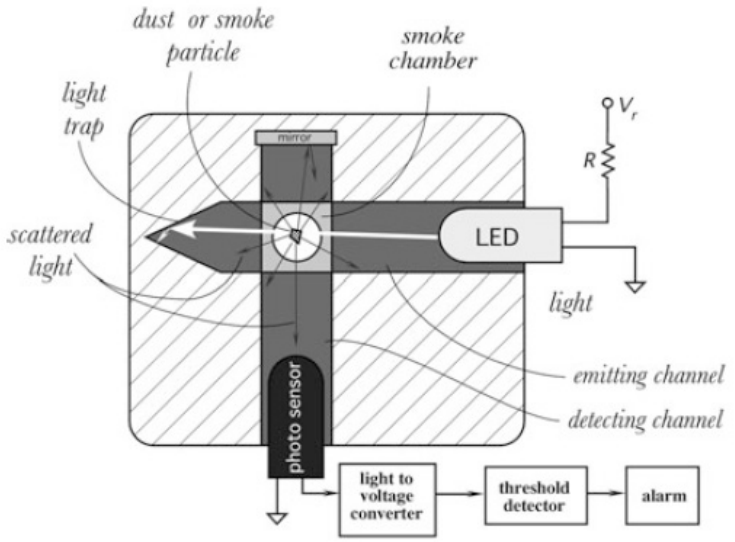

Fig. 11.23 Optical smoke detector

Optisk røykvarsler

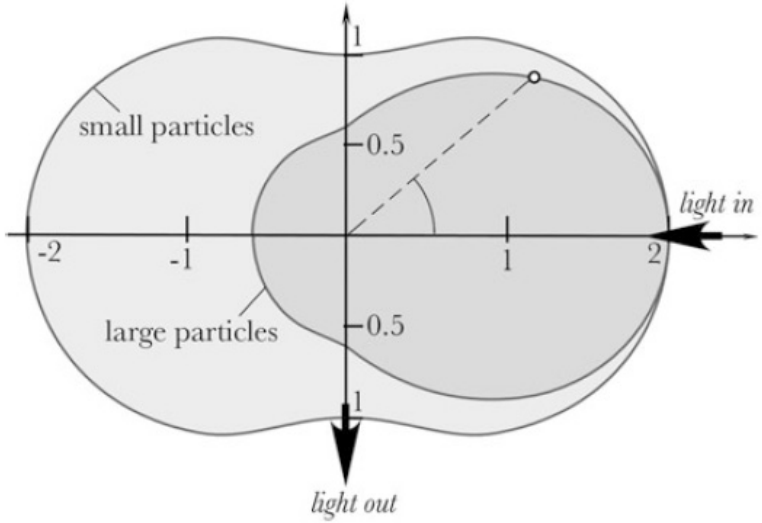

Fig. 11.24 Scattering directional diagram